Studies Towards Metabolically Stable Fluorine-18 Labelled Peptides and Their Efficient Syntheses

By

Brendan John Evans

Master of Radiopharmaceutical Science - 2017

Bachelor of Science (Major in Chemistry, Minor in Biomolecular Sciences) - 2016

Macquarie University, Australia

A Thesis Submitted in Partial Fulfillment of the Requirements for the Degree of

Master of Research

Department of Molecular Sciences

Macquarie University

Sydney, Australia

7th of June 2018

TABLE OF CONTENTS

DECLARATION

This work has not previously been submitted for a degree or diploma in any university. To the best of my knowledge and belief, the thesis contains no material previously published or written by another person except where due reference is made in the thesis itself.

Brendan John Evans

7th of June 2018

ACKNOWLEDGEMENTS

First of all, I am enormously thankful to my supervisor A/Professor Joanne Jamie who was always free to provide support, advice and positivity. I would like to especially thank A/Professor Andrew Katsifis for helping to formulate the idea for this project and continuing to provide valuable insight throughout the course of the project. I would also like to especially thank Dr Lidia Matesic for the invaluable support and input she provided during the project. I am also grateful to all the students and post-docs of both Joanne Jamie's and Ian Jamie's laboratories for their friendliness and willingness to help with any of my problems. I must also thank my family and friends, for the support and understanding they have ceaselessly provided me thought this project. Finally, I would like to thank Macquarie University for giving me this amazing opportunity to pursue this research in a field I am passionate about and for providing a stipend to help support me financially while performing this work.

ABSTRACT

Positron emission tomography (PET) is a powerful nuclear medicine imaging technique that has become invaluable for the *in vivo* diagnosis and staging of cancers and many other diseases. The overall aim of this project was to develop strategies for improving the metabolic stability and ease of synthesis of ^{18}F radiolabelled peptide conjugates for use in PET.

The first objective was to use model systems to determine if the substitution of an amide bond with a sulfonamide bond increases the metabolic stability of peptide conjugates. For this, *N*-benzoyl glycine and *N*-benzenesulfonyl glycine were incubated with the human carboxylesterase/amidase model enzyme pig liver esterase. Both compounds exhibited good stability, however, future work with other enzyme systems would be valuable.

The second objective was to synthesise a series of bifunctional aromatic and heteroaromatic compounds that possess the good leaving group tetramethylammonium (TMA) and an activated 4-nitrophenyl ester to enable efficient fluorination and peptide conjugation. Unfortunately, the 4-nitrophenyl ester proved to be too active, making it difficult to form the TMA activated aromatic systems. As a result, a new method was developed based upon the synthesis of TMA methyl esters. Using this method, the synthesis of a TMA bearing methyl ester was successfully trialled.

CHAPTER ONE

Introduction

This chapter introduces positron emission tomography (PET) and the vital role it plays in the diagnosis and staging of cancer. It also describes current trends towards radiolabelling peptides for use in PET, their significant advantages and the challenges that need to be overcome to develop and employ them. The specific objectives of the research conducted are also included.

1.1 Introduction

The ways in which cancers are diagnosed and treated are becoming increasingly more directed and specific. This has primarily been achieved through the identification and exploitation of characteristic tumour biology and biological targets that are uniquely expressed or significantly over-expressed in tumour cells. Due to this, molecular imaging technologies that utilise highly specific molecular probes such as positron emission tomography (PET) have become indispensable in the field of oncology.

Fluorine-18 is the most widely used radioisotope for clinical PET imaging. The well-known radiopharmaceutical, 2-deoxy-2-[^{18}F]fluoro-D-glucose ([^{18}F]FDG), is used in approximately 90% of all PET procedures.[1] This has often led to PET becoming synonymous to the study and use of [^{18}F]FDG. However, despite the dominance of [^{18}F]FDG, its use is suboptimal since it is not cancer specific and it also accumulates in various normal tissues. Due to this, there are an increasing number of new specific and selective molecular imaging agents being developed that are of potential medical interest.

The use of radiolabelled peptides as imaging agents is of growing interest due to the overexpression of many selective peptide receptors on the surface of tumour cells. Additionally, the increasing availability of highly active no-carrier-added [^{18}F]fluoride, combined with its near ideal properties, makes the radiofluorination of biomolecules such as peptides attractive. The result of this is the increasing need to develop facile methods for the conjugation of fluorine-18 to various peptides.

This thesis describes a potential method for increasing the stability of the labelled peptide systems and the development and comparison of methodologies for the direct one-step fluorination of biologically relevant peptides.

This chapter provides the theory behind positron emission tomography, introduces peptide-based radiotracers, methods for radiolabelling peptides, and the stability of radiolabelled peptides *in vivo*, and describes the objectives of the research work conducted during this Master of Research project.

1.1.1 Positron Emission Tomography

Positron (β^+) emission tomography (PET) is a nuclear medicine imaging technique for the non-invasive quantitative measurement of specific biochemical, physiological and pharmacological processes *in vivo*.[2] PET is useful in the diagnosis and staging of neurological and cardiovascular diseases and various cancers.[3]

PET involves administering a patient or animal with relatively short-lived positron-emitting radioisotopes. These radioisotopes are typically administered as part of a larger molecule, being either incorporated directly into its structure or linked to a functional group on its structure (**Figure 1.1**). Upon administration, the radioisotopes ideally accumulate in specific organs and/or tissues, as determined by the design of the radiopharmaceutical as a whole.[4]

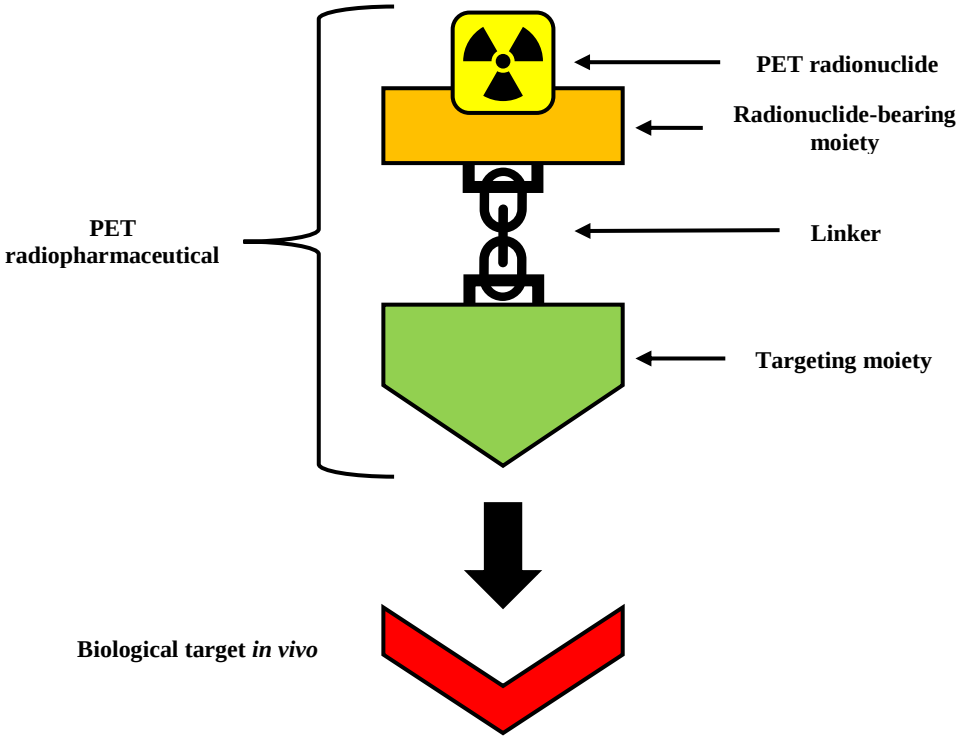

Figure 1.1. The structural components of PET radiopharmaceuticals.

The radionuclides used in PET imaging are proton-rich and readily decay by positron emission. Positron emission involves one of the protons in the nucleus of the radionuclide being converted into a neutron while emitting a positron and an electron neutrino (v_e). For example, the decay of fluorine-18 to oxygen-18 *via* positron emission is shown below.

$$^{18}_{9}F \rightarrow {}^{18}_{8}O + \beta^+ + v_e$$

The positron emission decay pathway allows radionuclides to shed their excess positive charge and transform into a more stable atomic form. The high energy positron emitted travels up to a few millimetres into the surrounding tissue before it encounters its antiparticle, an electron (e^-), and undergoes an annihilation event. An annihilation event involves the mass of both the positron and electron being converted into pure energy in the form of two gamma ray photons with equal energies (511 keV), emitted at 180° away from each other (**Figure 1.2, A**). PET imaging is based upon the coincident detection of these two photons within a PET scanner (**Figure 1.2, B**), and the consequent retro-projection of all detected coincidence lines from all annihilation events, to build a 3D map of the localisation of the radiotracer.[5]

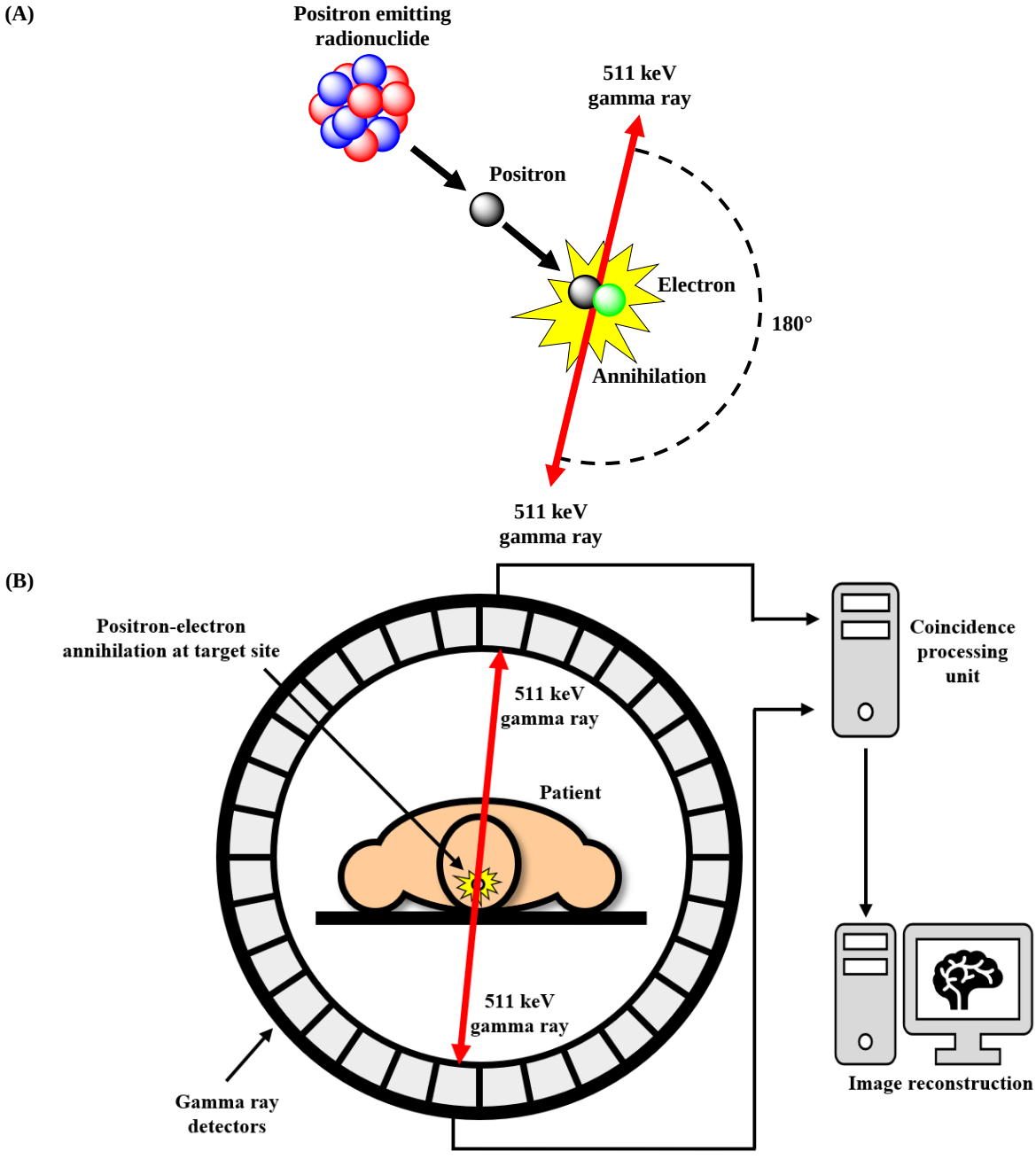

Figure 1.2. (A) Diagram of a positron-electron annihilation. (B) Diagram of a PET scanner.

1.2 Peptide Based Radiotracers

The last 20 years has seen an explosive growth in the development of radiolabelled peptides for targeted diagnostic imaging and therapy. While radiolabelled peptides have been applied to various molecular imaging modalities that use nuclear probes such as scintigraphy and single-photon emission computed tomography (SPECT), the superior image quality and quantitative data available from PET has resulted in a significant amount of research being devoted to the development of PET radiolabelled peptides.[6] Recently, [^{68}Ga]DOTATATE, also known as NETSPOT (**Figure 1.3**), received regulatory approval from the Food and Drug Administration (FDA). This is a significant milestone for the field as it is the first radiolabelled peptide for PET to be approved by the FDA.[7]

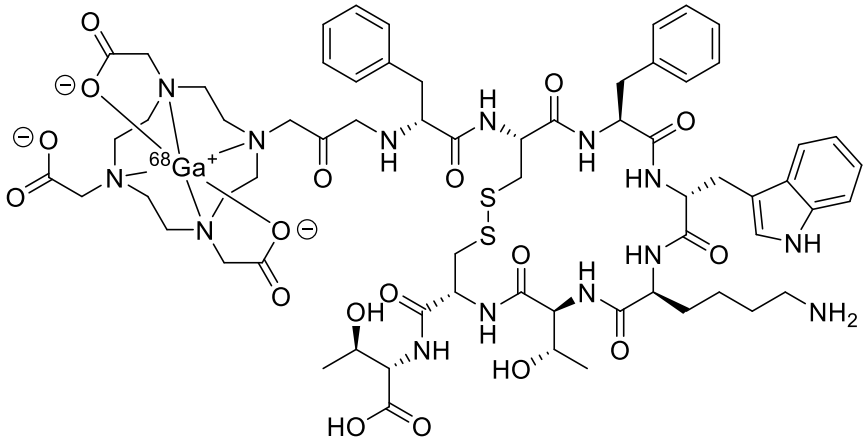

Figure 1.3. Structure of [^{68}Ga]DOTATATE (NETSPOT).

There are many advantages presented by using peptides as the specific targeting vectors of radiotracers. Primarily, there is a higher density of peptide receptors on tumour cells than in normal tissues, thus specific receptor-binding radiolabelled peptides can be designed to enable the efficient visualisation of various tumours.[8] Due to the small size of peptides, they often exhibit rapid pharmacokinetics, the ability to efficiently penetrate tumours, rapid clearance from the bloodstream and non-target tissues, and are not immunogenic.[8–11] Furthermore, peptides can be readily synthesised using conventional peptide synthesisers and any desired modifications to the structure can be engineered by making the appropriate changes to the peptide sequence during synthesis and/or by adding other structural modifications after synthesis, so long as the binding motif is preserved.[12–14]

The vast majority of radiolabelled peptides for PET imaging have been designed for use in oncology, and this orientation of the field towards oncology is reflected across recent review articles.[15–17] This focus is because various receptors known to bind specific peptide ligands are also known to be over-expressed in tumour cells, and thus make attractive targets for oncological PET imaging. G-protein-coupled receptors (GPCRs) are a class of receptors that are particularly well utilised in this regard. GPCRs function to detect extracellular signals in the form of specific ligands and to relay these signals

into the cell in a process that ultimately leads to a cellular response.[8] Several families of GPCRs have been found to be over-expressed in tumour cells, and consequently numerous methods have been developed for targeting these receptors with radiolabelled peptides.[18] Some commonly targeted peptides and their receptors for the development of radiopeptides are shown in **Table 1.1**. While not a receptor, prostate-specific membrane antigen (PSMA) is another target of interest in oncology as it is significantly over-expressed in prostate cancer cells compared to healthy prostate cells, making it an ideal target for the diagnosis and staging of prostate cancer.[19] Consequently, several radiolabelled ligands that target PSMA have been developed.[20,21]

Table 1.1. Common peptides, their receptors over-expressed in tumour cells, and the tumours they can be used to target.[6,16,17]

Peptide	Main receptor/s over-expressed in tumour cells	Tumour Target(s)
Somatostatin	Somatostatin receptor 2 (SST_2)	Neuroendocrine system, brain, breast, small cell lung cancer, kidney, lymphatic system
Bombesin/gastrin-releasing peptide	Bombesin receptor 2 (BB_2), gastrin-releasing peptide receptor (GRP-R)	Prostate, breast, gastric, colon, pancreatic, lung
Epidermal growth factor	Epidermal growth factor receptor (EGFR)	Breast
RGD	αvβ3-Integrin	Brain, ovary, breast, skin, lung, prostate
Neurotensin	Neurotensin 1 receptor (NTR_1)	Prostate, pancreas, brain, breast, colon, lung
α-Melanocyte-stimulating hormone (α-MSH)	Melanocortin-1 receptor (MC1R)	Skin
Vasoactive intestinal peptide (VIP)	Vasoactive intestinal peptide receptor 1 (VPAC1)	Neuroendocrine system, breast, stomach, liver, prostate
Exendin	Glucagon-like peptide-1 receptor (GLP-1)	Brain, ovary, prostate, thyroid, adrenal gland, pancreas
Cholecystokinin (CCK)/gastrin	Cholecystokinin-B/gastrin receptor (CCK-B)	Thyroid, brain, ovary, gastrointestinal system, lung

1.3 Methods for Radiolabelling Peptides

Among the most available radionuclides for PET, fluorine-18 (^{18}F), copper-64 (^{64}Cu), and gallium-68 (^{68}Ga) are the most applicable for radiolabelling peptides as their half-lives are in line with the biological half-lives of most peptides. Although direct radiolabelling of a peptide is possible, it presents significant challenges. As a result, the two most widely seen methods for the introduction of a radionuclide into a peptide are indirect methods that involve the use of either bifunctional metal chelators or prosthetic groups. Bifunctional metal chelators are molecules that contain a metal-

binding functionality, which can be bound to a peptide of choice to allow it to be radiolabelled with a radioactive metal ion (radiometal). Prosthetic groups are small molecules that are first radiolabelled before being attached to a peptide.

1.3.1 Labelling Peptides with Radiometals

Radiometals have long played a key role in nuclear medicine, with technetium-99m and its use in SPECT being the most well-known. Radiometals can be readily attached to biologically active molecules such as peptides using bifunctional metal chelators. Consequently, the use of bifunctional metal chelators for the conjugation of radiometals to peptides is well documented for SPECT imaging (^{99m}Tc), PET imaging (^{68}Ga or ^{64}Cu), and for radiotherapy (^{111}In, ^{177}Lu and ^{90}Y).[22] A major challenge faced when using bifunctional metal chelators is that they can introduce significant structural perturbations to the peptide, which can potentially disrupt receptor binding.[23]

1.3.2 Labelling Peptides with Fluorine-18

Over the last 10 years, the superior imaging characteristics, decreasing cost, increasingly wide availability, and larger production capacity of ^{18}F, have made radiolabelling of peptides with fluorine-18 a more attractive alternative to radiometal labelling of peptides. Consequently, there has been an increasing number of fluorine-18 labelled peptides reported.[15]

Despite the many favourable properties of ^{18}F for peptide radiolabelling, the direct radiofluorination of peptides presents considerable challenges. The primary challenge faced is that the conventional methods for ^{18}F-labelling are typically conducted at high temperatures and under basic conditions. These conditions are too harsh for most peptides and can cause the decomposition of the sensitive biomolecule, thus disrupting its biological activity.[24] An additional challenge is that any acid side chains in a target peptides' backbone may interfere with direct nucleophilic radiofluorination reactions.[11] These challenges have resulted in the development of indirect methods for the radiofluorination of peptides such as the use of various prosthetic group methodologies. However, the field of radiolabelling has taken large strides in recent years and various strategies for the direct radiofluorination of peptides have also been developed.[25–32]

1.3.2.1 Properties of Fluorine-18

Fluorine-18 exhibits a high positron emission efficiency of 97%. This is critical for PET imaging since only positron emissions result in the annihilation events that are detected by the PET scanner. Fluorine-18 has a half-life of 109.8 min, which is longer than the half-lives of other cyclotron produced positron-emitting radioisotopes (*e.g.* 20.4 minutes for carbon-11, 9.97 minutes for nitrogen-13, and 2.04 minutes for oxygen-15).[33] This longer half-life is favourable as it allows for longer, more complex syntheses to be performed, and use of longer scanning times that enables slower

physiological processes to be imaged.[34] Additionally, the longer half-life permits the transport of fluorine-18 labelled compounds to facilities and hospitals that do not have access to a cyclotron. Moreover, the half-life of fluorine-18 is still relatively short, which helps to minimise the radiation dose to patients.

The relatively low positron energy of 633 keV produced by the decay of ^{18}F as compared to 1920 keV for ^{68}Ga, results in a PET image with a higher spatial resolution, as the generated positron travels a shorter maximum distance prior to annihilation in the target tissue (0.42 mm in compact bone, 0.54 mm in soft tissue, 0.58 mm in adipose tissue and 1.52 mm in lung tissue).[35]

An additional advantage of fluorine-18 is that a fluorine atom is sterically similar to a hydrogen atom (Van der Waals radius: 1.2 A° for H and 1.35 A° for F) and can thus replace a hydrogen atom on a target molecule without significantly changing the properties of the molecule.[36] Due to this, fluorine-18 can be potentially used to convert any biologically active molecule into a PET probe without severely changing the molecules' affinity for the molecular target. This is a distinct advantage when compared to the significant structural change that comes from use of large chelating groups that must be attached to molecules to accommodate the incorporation of radiometals.

1.3.2.2 Production of Fluorine-18

Fluorine-18 is readily produced in cyclotrons from a variety of nuclear reactions involving the bombardment of a target with accelerated particles. The differences in these nuclear reactions comes from the choice of target material, which can be gas or liquid, and the choice of accelerated particles, most often protons or deuterons. These choices allow for fluorine-18 to be produced in two distinct chemical forms, electrophilic [^{18}F]-fluorine and nucleophilic [^{18}F]-fluoride. The availability of both electrophilic and nucleophilic fluorine-18 allows for a wide variety of radiofluorination reactions to be performed. Additionally, the relatively low energy photon beam required for the production of fluorine-18 is readily achievable from small, so called "medical" cyclotrons, which can regularly produce 50-100 GBq (gigabecquerel) batches of [^{18}F]F^- or [^{18}F]F_2 within 30-60 minutes.[37] This has allowed for a growing number of sites around the world to gain access to fluorine-18 radiopharmaceuticals.

A significant difference between the two forms of fluorine-18 is their molar activities and if carrier was added in their preparation. The molar activity of a radioisotope or radiolabelled compound is the measure of its radioactivity (often expressed in becquerels) per molar amount (Bq/mol).[38] For radioactive preparations involving fluorine-18, the molar activity reflects the extent to which the ^{18}F-labelled compound is contaminated with non-radioactive ^{19}F-labelled compound, where a lower

molar activity indicates a greater amount of the ^{19}F-labelled compound being present in the preparation.

No-carrier added indicates that no carrier in the form of the non-radioactive isotope has been intentionally added during the preparation of a radioisotope or radiochemical synthesis. This results in a higher molar activity being achievable as there is less risk of the non-radioactive isotope being incorporated into the preparation.[38]

High molar activity is very important in the preparation of receptor-binding PET radiopharmaceuticals, as the targeted receptors are often only present in low concentrations and are thus easily saturated. For example, the preparation of PET radiopharmaceuticals with high molar activities allows these radiopharmaceuticals to be administered at levels where they will only occupy a small percentage of the total available target binding sites. If the PET radiopharmaceutical is prepared with a low molar activity, more of it must be administered, which can result in significant saturation of the target binding sites. This is associated with decline in signal to noise ratios, and may additionally result in pharmacological or toxic effects.[39]

Electrophilic fluorine-18

There are two main methods utilised to produce electrophilic fluorine-18. The original method involves the ^{20}Ne(d, α)^{18}F nuclear reaction, which proceeds *via* the bombardment of a target gas of ^{20}Ne (and ~0.1-2% $^{19}F_2$ as carrier) with deuterons, to produce fluorine-18 as [^{18}F]F_2 gas.[40] This method has been superseded by the ^{18}O(p, n)^{18}F nuclear reaction, which proceeds *via* the bombardment of a target of enriched $^{18}O_2$ gas with protons, to produce fluorine-18 which sticks to the walls of the target.[41] After the remaining $^{18}O_2$ gas is recovered, the target is filled with a mixture of noble gas and [^{19}F]F_2 and irradiated again to trigger isotopic exchange between the adsorbed fluorine-18 and the added [^{19}F]F_2 to produce [^{18}F]F_2 gas.[41] The produced [^{18}F]F_2 gas can then be used directly for electrophilic radiofluorination, or it can be converted into other electrophilic fluorination reagents. The use of unlabelled [^{19}F]F_2 gas in both of these methods results in the production of carrier-added [^{18}F]F_2 gas (consisting of both [^{18}F] and [^{19}F] isotopes), with a relatively low molar activity of 0.1-0.6 GBq/μmol.[42]

Nucleophilic fluorine-18

Nucleophilic fluorine-18 is readily produced *via* the ^{18}O(p, n)^{18}F nuclear reaction, by the bombardment of a target of [^{18}O]H_2O enriched water with protons.[43] This produces nucleophilic fluorine-18 as [^{18}F]fluoride ions in aqueous solution. In contrast to the production of electrophilic [^{18}F]F_2, the production of nucleophilic [^{18}F]fluoride has no carrier gas added. As a result,

radiolabelled compounds prepared from [^{18}F]fluoride can be produced with a molar activity of ~100 GBq/µmol, which is much higher than those prepared from [^{18}F]F_2.[42] Thus, due to its far superior molar activity over electrophilic [^{18}F]F_2, nucleophilic [^{18}F]fluoride is generally preferred for the preparation of radiotracers. It should be noted however that while lower molar activity radiopharmaceuticals synthesised using electrophilic fluorine-18 can be tolerated for targeting metabolic markers, receptor mediated radiopharmaceuticals (such as those based on peptides) require molar activities that are only attainable from nucleophilic fluorine-18.[39]

1.3.2.3 Radiofluorination Reactions with Nucleophilic Fluorine-18

While the [^{18}F]fluoride ion is a strong nucleophile, there a two major challenges that must be addressed to utilise it efficiently. The first challenge is that in an aqueous solution, the [^{18}F]fluoride anion readily forms a tight hydration shell with surrounding water molecules, rendering itself inactive towards nucleophilic substitution.[44] Consequently, reaction schemes involving nucleophilic [^{18}F]fluoride generally require the strict exclusion of water and often include azeotropic drying with acetonitrile, in addition to the almost exclusive use of aprotic polar organic solvents (*e.g.* acetonitrile, dimethyl sulfoxide, dimethylformamide).[45] Several publications have recently successfully demonstrated nucleophilic [^{18}F]fluoride substitution using the polar protic solvents *t*-butanol and *t*-amylalcohol[44,46], and there have also been publications that have demonstrated an enhanced yield when a small percentage of water was added to the reaction.[47]

The second challenge is that the solubility and nucleophilicity of the [^{18}F]fluoride anion in the organic solvent system of the nucleophilic substitution reaction must also be considered. To address this, highly nucleophilic [^{18}F]fluoride systems that are soluble in aprotic polar organic solvent are generated through the addition of bulky phase transfer catalysts prior to the evaporation of water. These systems include alkali metal (K, Cs, Rb) [^{18}F]fluoride/cryptand (Kryptofix 2.2.2) complexes (*e.g.* [^{18}F]KF/Kryptofix[2.2.2]) and quaternary ammonium [^{18}F]fluoride derivatives (*e.g.* tetrabutylammonium [^{18}F]fluoride).[48]

The generation of the reactive [^{18}F]fluoride ion allows for a variety of methods to be applied for its introduction to aliphatic and aromatic compounds. The diversity in nucleophilic radiofluorination reactions is achieved through the application of a wide variety of leaving groups, substrates and reaction conditions.

1.3.3 Labelling Peptides with Fluorine-18 Using Prosthetic Groups

Prosthetic groups are the most common method used for the synthesis of ^{18}F-labelled peptides. Prosthetic groups are small molecules that contain both a functional group that allows for the introduction of fluorine-18, and a second functional group that allows for its bioconjugation to a

peptide. Prosthetic group labelling of a peptide typically requires two steps. Initially fluorine-18 is introduced to the prosthetic group typically *via* nucleophilic substitution, then the ^{18}F-labelled prosthetic group is conjugated to the target peptide. The subsequent purification of the product *via* HPLC or solid phase extraction to remove any unlabelled peptide and/or by-products ensures a high molar activity of the ^{18}F-labelled peptide.[49] The use of prosthetic groups allows peptides to be labelled with fluorine-18 using reaction conditions that do not diminish the biological activity of the peptide. This is because a prosthetic group can withstand harsh radiofluorination reaction conditions that may otherwise cause a peptide to be hydrolysed, and hence, the peptide only needs to be exposed to the mild reaction conditions required for the conjugation of ^{18}F-labelled prosthetic group to the peptide. The majority of prosthetic groups are designed to conjugate to a peptide by reacting with either the amine or thiol functional groups inherent to peptides *via* acylation, alkylation, amidation, imidation, oxime, or hydrazone formation (**Figure 1.4**).[50–52]

Amine-reactive prosthetic groups.

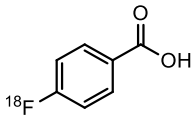

[^{18}F]FBA
4-[^{18}F]fluorobenzoic acid

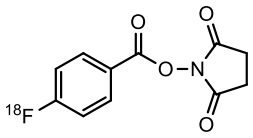

[^{18}F]SFB
N-succinimidyl-4-[^{18}F]fluorobenzoic acid

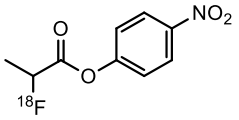

[^{18}F]NFP
4-nitrophenyl-2-[^{18}F]fluoropropionate

Thiol-reactive prosthetic groups.

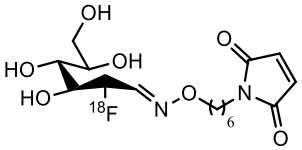

[^{18}F]FDG-MHO
[^{18}F]FDG-maleimidehexyloxime

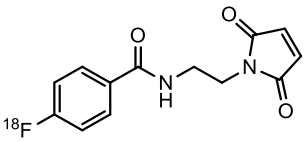

[^{18}F]FBEM
N-[2-(4-[^{18}F]fluorobenzamido)ethyl]maleimide

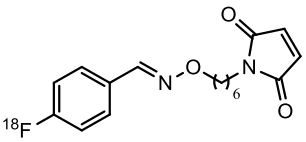

[^{18}F]FBAM
N-[6-(4-[^{18}F]fluorobenzylidene)aminooxyhexyl]maleimide

Figure 1.4. Examples of amine-reactive and thiol-reactive prosthetic groups.

Another class of prosthetic groups that has been developed contains the functional groups required for various click chemistry reactions and can subsequently be conjugated to properly functionalised peptides (**Figure 1.5**).[53,54]

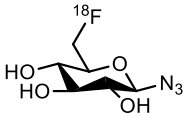

[^{18}F]GlcA
6-deoxy-6-
[^{18}F]fluoroglucosylazide

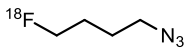

[^{18}F]BuA
6-[^{18}F]fluoro-2-
ethynylpyridine

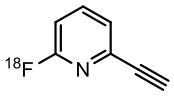

[^{18}F]FEP
6-[^{18}F]fluoro-2-ethynylpyridine

Figure 1.5. Examples of click chemistry based prosthetic groups

1.3.4 Direct Labelling of Peptides with Fluorine-18

For direct radiolabelling, an unlabelled bifunctional activating group is initially attached to the peptide, then the resulting conjugated system is radiofluorinated under mild reaction conditions that are amenable to peptides. In this way, direct labelling methodologies allow for biologically relevant peptides to be labelled with fluorine-18 in a single time-efficient step, and thus a higher molar activity can be achieved.

The first moieties developed for direct radiofluorination were based off the well-developed fluorobenzoic acid prosthetic group and aimed to make the conjugated peptide system highly activated towards nucleophilic aromatic substitution (**Figure 1.4**). This involves the conjugation of a free amine on the target peptide with a disubstituted benzoic acid containing a good leaving group such as trimethylammonium (TMA) or NO_2 in the *para*-position, and an electron-withdrawing group such as CN or CF_3 in the *meta*-position, to activate the benzene ring for nucleophilic substitution.[55,56] Pyridine derivatives with TMA *ortho* to the pyridinyl nitrogen have also been found to be sufficiently activated for nucleophilic substitution (**Figure 1.6**).[56] A benefit of these methods is that they can be easily applied to other peptides that have been previously labelled using prosthetic group methodologies, to reduce the number of synthetic steps required to produce the ^{18}F-labelled peptide.

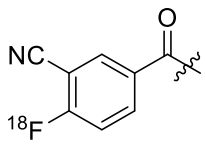

3-CN-4-[^{18}F]FBz

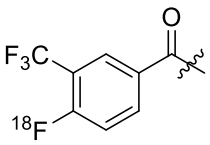

3-CF_3-4-[^{18}F]FBz

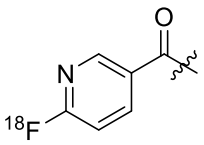

6-[^{18}F]FPy

Figure 1.6. Examples of aromatic nucleophilic substitution based ^{18}F-labelled peptide conjugates prepared using direct labelling strategies.

Several methods that use silicon-fluoride, boron-fluoride or aluminium-fluoride acceptor chemistry for the ^{18}F-labelling of biologically useful peptides have been developed.[25–32] These methods utilise the high affinity of silicon, boron and aluminium to fluorine and their facile isotopic exchange of ^{19}F with ^{18}F following the conjugation of silicon, boron and aluminium to peptides. Examples of silicon-fluoride acceptor and boron-fluoride acceptors are provided in **Figure 1.7** and aluminium-fluoride-peptide conjugates in **Figure 1.8**. Both the Si-F and B-F bonds do suffer from hydrolysis *in vivo*.[57] While significant advances have been made to alleviate this,[27,28,57,58] they are still not ideal for *in vivo* imaging.[57]

Silicon-Fluoride Acceptors (SiFA)

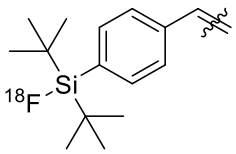

[^{18}F]SiFA

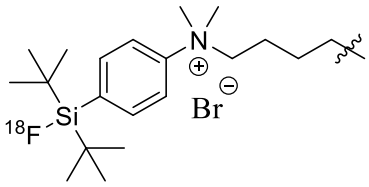

[^{18}F]SiFA*lin*

Boron-Fluoride Acceptors (RBF_3^-)

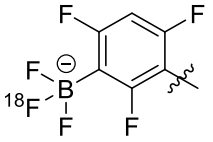

[^{18}F]ArBF_3

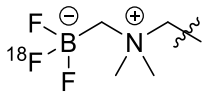

[^{18}F]AmBF_3

Figure 1.7. Examples of silicon-fluoride acceptor and boron-fluoride acceptor based ^{18}F-labelled peptide conjugates prepared using direct labelling strategies.

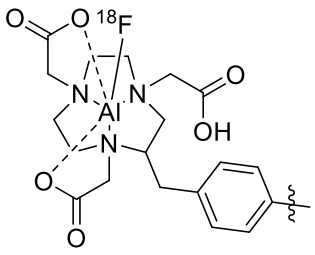

[^{18}F]AlF-NOTA

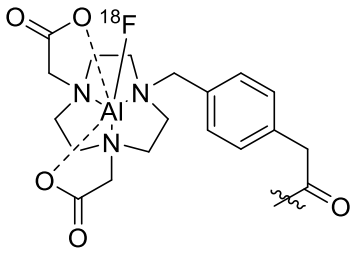

[^{18}F]AlF-NODA

Figure 1.8. Examples of aluminium-fluoride acceptor based ^{18}F-labelled peptide conjugates prepared using direct labelling strategies.

1.4 Metabolic Stability of Fluorine-18 Labelled Radiopharmaceuticals

One of the most important features to consider in the designing of a radiolabelled peptide is its stability *in vivo*. Unmodified peptides often present very short biological half-lives due to rapid proteolysis in the blood, kidneys, or liver.[59] This short half-life is a significant challenge for the successful application of peptide based radiopharmaceuticals *in vivo* since the bulk of the radiolabelled peptides may be degraded before they reach the target. This is a major problem as the desired target will not be properly imaged, and any radiolabelled metabolites will show non-target binding, which will further diminish the imaging results. Consequently, most peptides for use in radiopharmaceuticals must be synthetically modified to minimise metabolic degradation *in vivo*.[9,60] For example, the native peptide somatostatin presents an *in vivo* half-life of approximately 2-3 minutes, however its synthetic peptide derivative, octreotide, presents a half-life of approximately 90 minutes, which is long enough for clinical applications (**Figure 1.9**).[61]

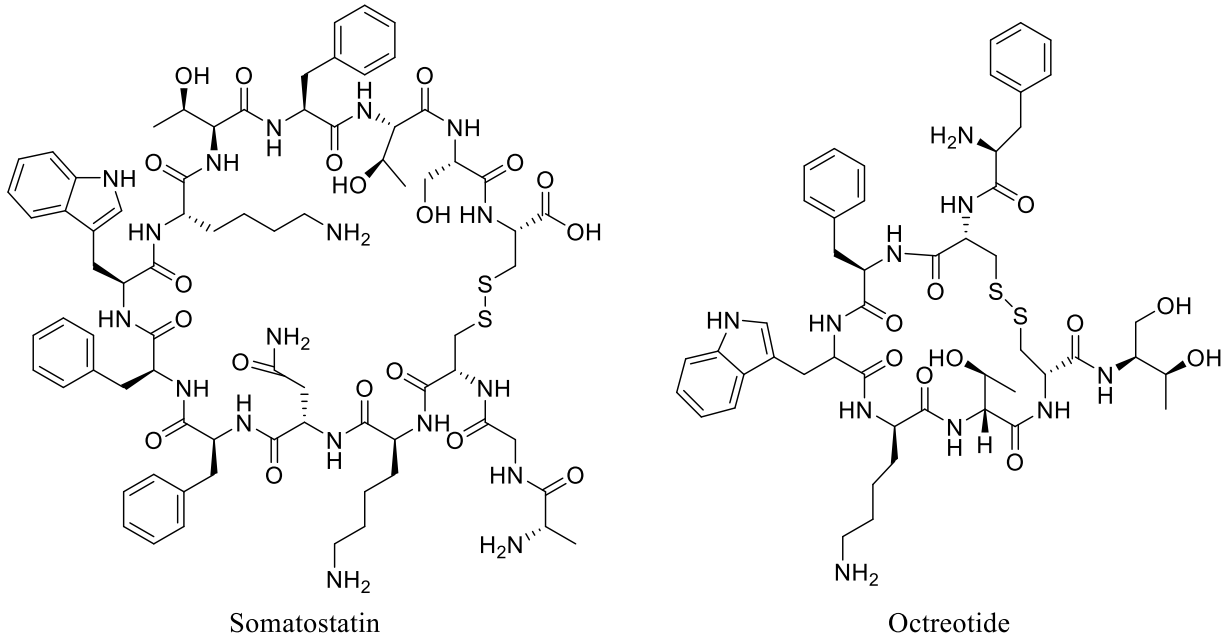

Figure 1.9. Structures of somatostatin and octreotide.

1.4.1 Radiodefluorination of Fluorine-18 Labelled Compounds

Radiodefluorination is a major issue for some ^{18}F-radiotracers *in vivo*, and involves the cleavage of [^{18}F]fluoride from the radiotracer, resulting in the release of free [^{18}F]fluoride ions into the bloodstream. The [^{18}F]fluoride ions produced by radiodefluorination readily accumulate into the calcium-rich fluorophilic bones of the body.[62] Consequently, radiodefluorination of radiotracers *in vivo* presents a significant hinderance to imaging as it leads to a degradation of signal to noise ratio that can obscure the imaging results.[63] This is especially problematic while imaging the brain, as any [^{18}F]fluoride bound to the skull can make the quantitation of radiotracer binding in the brain highly inaccurate.[64]

In general, radiotracers that possess [^{18}F]fluoride bound to an aliphatic carbon are more prone to radiodefluorination, while radiodefluorination can generally be avoided by binding the [^{18}F]fluoride to an aromatic carbon within a phenyl or pyridinyl group.[64] This is consistent with the knowledge that aromatic $C_{Ar}(sp^2)$-F bonds are stronger than aliphatic $C(sp_3)$-F bonds.[65] Thus, to minimise the risk of radiodefluorination, the radiofluorination of aromatic systems is favoured over aliphatic systems.

1.4.2 Stability of Radiolabelled Peptides *In Vivo*

There are several strategies that can be applied to stabilise peptides against proteolysis, such as protecting the *N*- and/or *C*-terminus, substituting L-amino acids with D-amino acids, modification of amino acids, cyclisation and conjugation to macromolecules.[9,66] Since the proteolysis of peptides involves the enzymatic cleavage of amide bonds by proteases or peptidases[67], the stability of a peptide can also be improved by substituting amide bonds with other bond types that are either intrinsically more stable or are not recognised by the relevant enzymes.[66] An example of this is the sulfonamide bond, which can be considered metabolically inert.[68] Recent work by Löser *et al*. has shown that the amide *N*-(4-fluorophenyl)-fluoroacetanilide is less stable when treated with pig liver esterase (PLE, the porcine homologue of carboxylesterase) than the sulfonamide analogue *N*-(4-fluorophenyl)-3-fluoropropane-1-sulfonamide (**Figure 1.10**).[69] They found that after 120 minutes, only 20% of *N*-(4-fluorophenyl)-fluoroacetanilide, remained intact, while at the same time point, over 95% of the *N*-(4-fluorophenyl)-3-fluoropropane-1-sulfonamide, remained intact. While, these compounds weren't complete structural analogues of each other, this research provides support for sulfonamides improving the metabolic stability of radiopharmaceuticals and other amide bearing drugs.

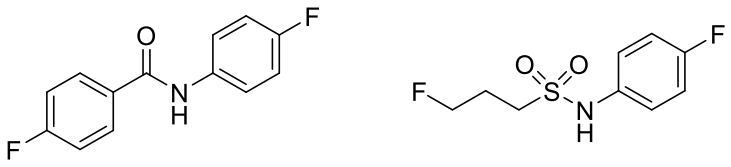

N-(4-fluorophenyl)-fluoroacetanilide

N-(4 fluorophenyl)-3-fluoropropane-1-sulfonamide

Figure 1.10. Structure of *N*-(4-fluorophenyl)-fluoroacetanilide and *N*-(4-fluorophenyl)-3-fluoropropane-1-sulfonamide.

1.5 Objectives of This Thesis

The overall goal of this research is to ultimately develop metabolically stable fluorine-18 labelled peptides that can be efficiently synthesised for use in PET imaging. To achieve this goal, a series of compounds that are highly activated under mild conditions towards both peptide conjugation and subsequent radiofluorination must be designed and synthesised. Due to the limited 10-month timeframe of this Master of Research Degree, the research work presented in this thesis was dedicated to performing the initial steps required for the overall project.

The specific aims of this thesis were to i) perform a pilot metabolic stability study on model aromatic amide and sulfonamide analogues using a simple enzyme system; and ii) conduct preliminary studies towards the synthesis of aromatic prosthetic groups that would be highly activated towards both bioconjugation to a peptide at a free amine and subsequent incorporation of [^{18}F]fluoride by nucleophilic substitution.

CHAPTER TWO

Comparative Stability of Amide and Sulfonamide Model Systems

This chapter explores the results of preliminary experiments performed to determine if the sulfonamide bond can increase metabolic stability compared to an amide bond when linking radiotracers to peptides. The work in this chapter was performed in parallel to the work described in Chapter 3.

2.1 Introduction

As described in Chapter 1, the synthesis of many peptide-based radiopharmaceuticals has been achieved through the conjugation of aromatic prosthetic groups to the primary amine residue of a peptide (*N*-terminus or lysine) through the formation of amide (peptide) bonds. While this method has been convenient for many fluorine-18 radiolabelled pharmaceuticals, the resulting aromatic amides have been found to be unstable *in vivo* due to enzyme catalysed hydrolysis.[70] The exact enzymes involved in this metabolic process are not known, however, the participation of carboxylesterase (EC 3.1.1.1) is thought likely, along with other hydrolases.[68,71] Carboxylesterase, in addition to esterase activity, also presents some amidase activity, and is known to participate in the hydrolytic metabolism of many drugs including radiopharmaceuticals.[72,73]

The metabolic hydrolysis of sulfonamide bonds has not been well investigated. As described in Chapter 1, recent work by Löser and co-workers showed that the amide *N*-(4-fluorophenyl)-fluoroacetanilide is less stable when treated with pig liver esterase (PLE, the porcine homologue of carboxylesterase) than the sulfonamide analogue *N*-(4-fluorophenyl)-3-fluoropropane-1-sulfonamide (**Figure 1.10**).[69]

This chapter describes the research undertaken to further assess the potential benefit to metabolic stability of sulfonamides over amide groups by comparing *N*-benzoyl glycine against the sulfonamide analogue, *N*-benzenesulfonyl glycine, as a model system for an aromatic prosthetic group conjugated to a peptide.

2.1.1 Model System

Due to the cost of the precursors and biologically relevant peptide systems, and to reduce the number of variables, the initial proof of concept for these experiments was performed using model systems that could be cheaply and easily produced. To this end, the initial assessment of the metabolic stability was examined using the simplest aromatic amide and sulfonamide-amino acid conjugated systems, *N*-benzoyl glycine and *N*-benzenesulfonyl glycine, respectively, with pig liver esterase (**Figure 2.1**).

These compounds were proposed to allow for trends in metabolic stability to be established in an affordable and timely manner, before moving on to more sophisticated systems. Pig liver esterase (PLE) was chosen as a model enzyme for examination of metabolic stability of *N*-benzoyl glycine and *N*-benzenesulfonyl glycine due to PLE being an excellent model for human carboxylesterase, its use in the similar experiments of Löser *et al.*[69], and its affordability and stability. Cleavage of the glycine analogues with PLE would produce the products glycine, along with benzoic acid or benzenesulfonic acid for *N*-benzoyl glycine and *N*-benzenesulfonyl glycine, respectively (**Figure 2.1**). It was anticipated that the loss of the starting compounds and production of these hydrolysis products would be easily detected, allowing the rate of breakdown of *N*-benzoyl glycine and *N*-benzenesulfonyl glycine to be readily measured and compared.

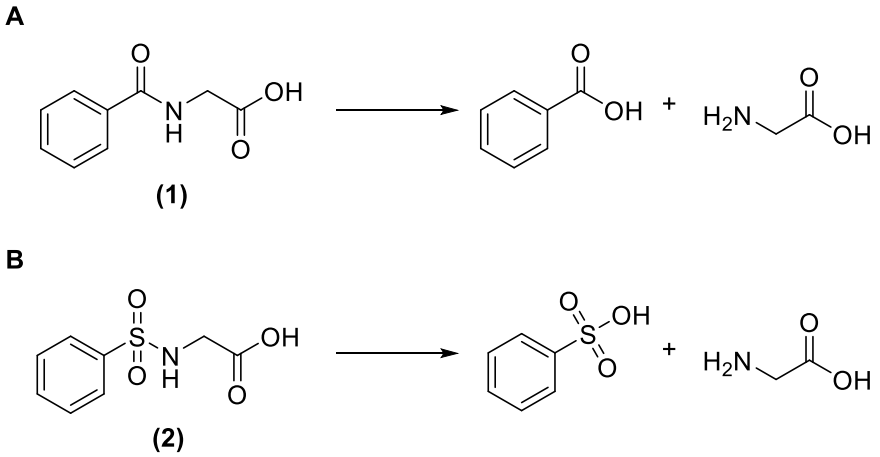

Figure 2.1. (A) Cleavage of *N*-benzoyl glycine **(1)** to benzoic acid and glycine. (B) Cleavage of *N*-benzenesulfonyl glycine **(2)** to benzenesulfonic acid and glycine.

2.2 Results and Discussion

2.2.1 Synthesis of Model Compounds

N-Benzoyl glycine **(1)** was successfully synthesised in an unoptimised yield of 49%, utilising the method of Weber *et al.*[74], through the condensation of benzoyl chloride with glycine in the presence of NaOH in 75% water and 25% dioxane. ^{1}H NMR and melting point data were in agreement with the literature.[74,75] *N*-Benzenesulfonyl glycine **(2)** was similarly synthesised by condensation of benzenesulfonyl chloride with glycine in the presence of aqueous NaOH in an unoptimised yield of 13%, utilising the method of DeRuiter *et al.*[76] ^{1}H NMR and melting point data were in agreement with the literature.[76] TLC monitoring of the reaction to form *N*-Benzenesulfonyl glycine indicated that all starting material had been consumed, but unlike in the literature, the product did not precipitate out upon acidification. The reaction mixture was therefore extracted into diethyl ether. This was likely inefficient due to partial solubility of the product in both the organic and aqueous solvents. Unfortunately, neither *N*-benzoyl glycine nor *N*-benzenesulfonyl glycine could be characterised by

mass spectrometry since Macquarie University's in-house LC-MS facilities were rendered unavailable during the time of this work.

2.2.2 Testing Enzyme Activity

To confirm the activity of the purchased batch of pig liver esterase, a spectrometric enzyme activity study was performed using the standard substrate *p*-nitrophenyl butyrate.[69,77] The formation of cleavage product was found to be highly linear over the first 3 minutes of the assay ($r^2 = 0.9886$). The assay gave a Michaelis constant (K_m) of 0.16 ± 0.02 mM (**Figure 2.2**), which was consistent with the literature value of 0.14 ± 0.02 mM.[77]

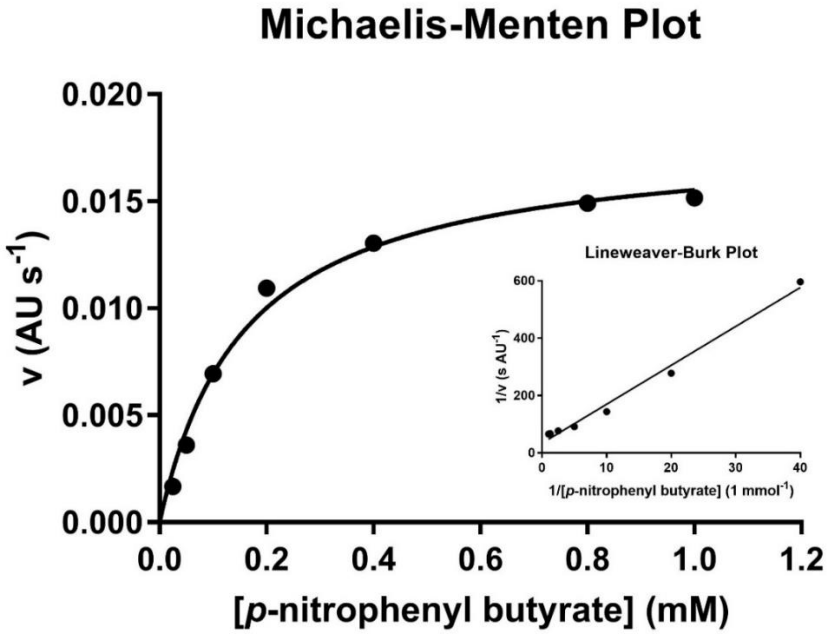

Figure 2.2. Michaelis-Menten plot used for the determination of Michaelis constant (K_m) of pig liver esterase towards *p*-nitrophenyl butyrate.

2.2.3 Testing Enzymatic Degradation of Amide *vs* Sulfonamide Compounds

To examine the stability of *N*-benzoyl glycine and *N*-benzenesulfonyl glycine against the pig liver esterase, a method adapted from the work of Löser *et al.*[69] and Vine *et al.*[78] was used. In this method, an assay solution for each of the compounds was prepared in 10 mM phosphate buffer at pH 7.4 and incubated with a range of PLE concentrations (20, 50 or 100 U/mL) at 37°C. Controls without PLE were also prepared and incubated in an identical manner.

It was initially anticipated that the rate of hydrolysis of *N*-benzoyl glycine and *N*-benzenesulfonyl glycine would be monitored in real time by UV-Vis in a manner similar to that of Vine *et al.*[78] However, it was found that any viable absorbance peak for either *N*-benzoyl glycine or *N*-benzenesulfonyl glycine was completely obscured by the absorbance of PLE, at any viable concentration of PLE, and the cleavage product of *N*-benzoyl glycine, benzoic acid, was also too

similar in absorbance to the starting compound (**Figure 2.3**). Benzenesulfonic acid could not be sourced during the research and thus its absorbance profile could not be obtained, though it was expected to be similar to that of benzoic acid.

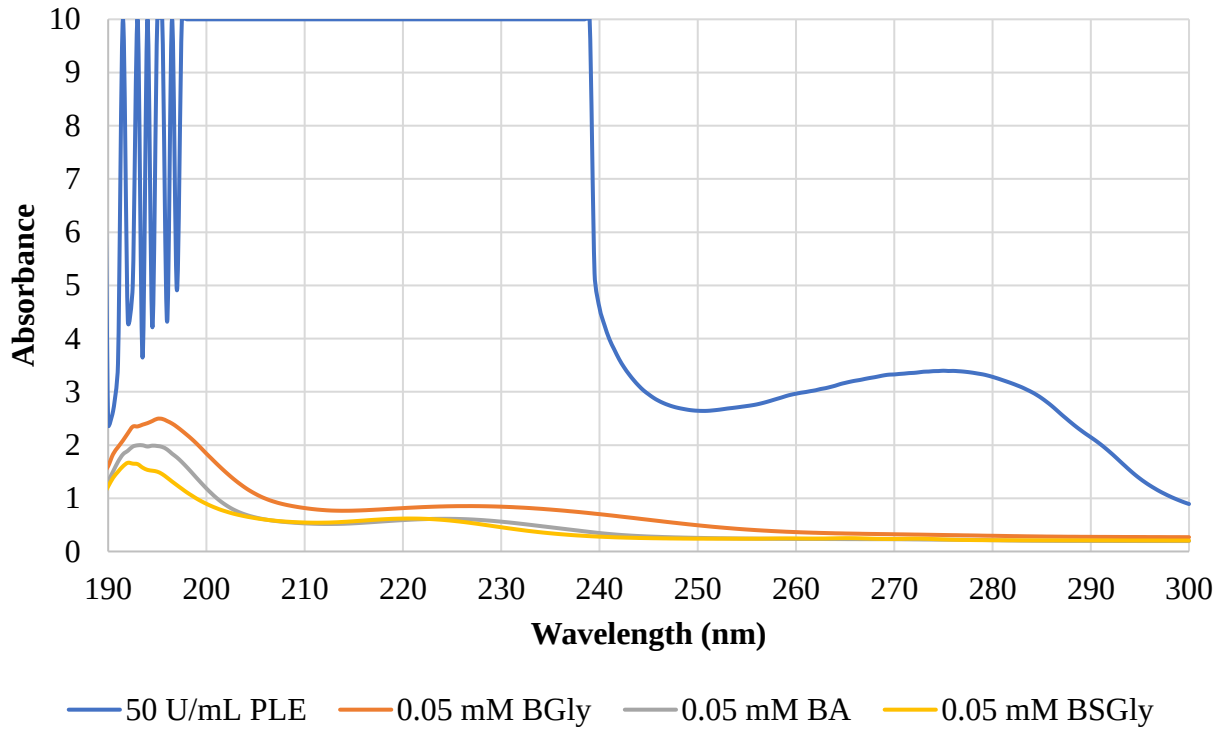

Figure 2.3. UV-Vis spectral profiles of *N*-benzoyl glycine (BGly), *N*-benzenesulfonic acid (BSGly), benzoic acid (BA) and pig liver esterase (PLE).

Löser *et al.* monitored the rate of cleavage in their experiments by taking aliquots of the assay solutions at set time intervals and quenching their enzyme activity immediately through the addition of TFA solution (2% in acetonitrile) such that the quenched samples were 1% in TFA (*v/v*). The quenched samples were then analysed by reversed phase HPLC for the presence of the starting material and its change in concentration over time. As a qualitative proof of concept, aliquots of the 1 mM *N*-benzoyl glycine and 1 mM *N*-benzenesulfonyl glycine incubation solutions (20, 50 or 100 U/mL PLE) were taken immediately following the addition of PLE to the incubation solutions and at 30 minute intervals up to 240 minutes, then quenched following Löser *et al.*'s procedure. Controls without PLE were also incubated, sampled and quenched in an identical manner.

A total incubation time of 240 minutes was chosen because it represents a time point greater than two half-lives of fluornine-18, which is more than enough time for most PET procedures post radiopharmaceutical injection. Therefore, the majority of fluorine-18 labelled radiopharmaceuticals would not have to be metabolically stable beyond this point. In most PET imaging studies, imaging occurs within 2 hours of administering the radiopharmaceutical, with the exact times varying greatly

between specific radiopharmaceuticals due to their different target uptake rates and thus the time taken to reach a sufficiently high target to nontarget radio. For example, when using [^{18}F]FDG optimal imaging results are obtained after approximately 60 to 90 minutes of uptake time, post radiopharmaceutical injection, prior to imaging.[79,80]

2.2.3.1 Sample Analysis by TLC

The quenched samples were analysed by reversed phase TLC and normal phase TLC for the presence of *N*-benzoyl glycine or *N*-benzenesulfonyl glycine and their respective hydrolysis products. The starting compounds, in addition to benzoic acid and benzenesulfonic acid, were expected to be readily visualised on the TLC plates at 254 nm, while glycine was expected to be detected with ninhydrin. TLC examination of the *N*-benzoyl glycine and *N*-benzenesulfonyl glycine samples with PLE present showed the appearance of a glycine spot, the size and intensity of which seemed to increase overtime. The appearance of glycine seemed to occur later for the *N*-benzenesulfonyl glycine samples compared to the *N*-benzoyl glycine samples, and when it did appear, it was less intense. Additionally, TLC examination of the controls (without PLE) did not appear to show any degradation of the compounds.

2.2.3.2 Sample Analysis by HPLC

With the results of the TLC examination looking promising, further analysis of the collected samples using reversed phase HPLC (PDA detection), in a method similar to that reported by Löser *et al*., was planned. This was initially planned to be done in-house at Macquarie University, however, due to unforeseen circumstances, the instrument was unavailable during the time it was required for this work. As a result, samples were sent for HPLC analysis at the Australian Nuclear Science and Technology Organisation (ANSTO). Due to the cost involved, unfortunately only the incubation samples with the highest PLE concentration of 100 U/mL and the controls with no PLE were able to be analysed. Representative HPLC spectra are shown in the Appendix 1.

The peak area of the starting materials (*N*-benzoyl glycine or *N*-benzenesulfonyl glycine) for the incubation experiments with 0 U/mL and 100 U/mL PLE were measured for each 30 minute time point over the 240 minutes at 225 nm. The data from these analyses were expressed as relative peak area (A/A_0) *vs* time (where A = peak area of the sample and A_0 = peak area of the sample at time zero). The relative peak areas of *N*-benzoyl glycine over time across the two conditions tested is shown in **Figure 2.4**. For this analysis, the 30 minute time point for the 100 U/mL PLE sample was a significant outlier and thus not included. The relative peak area of *N*-benzenesulfonyl glycine over time across the two conditions tested is shown in **Figure 2.5**. A comparison of the relative peak areas of *N*-benzoyl glycine in comparison to *N*-benzenesulfonyl glycine is shown in **Figure 2.6**.

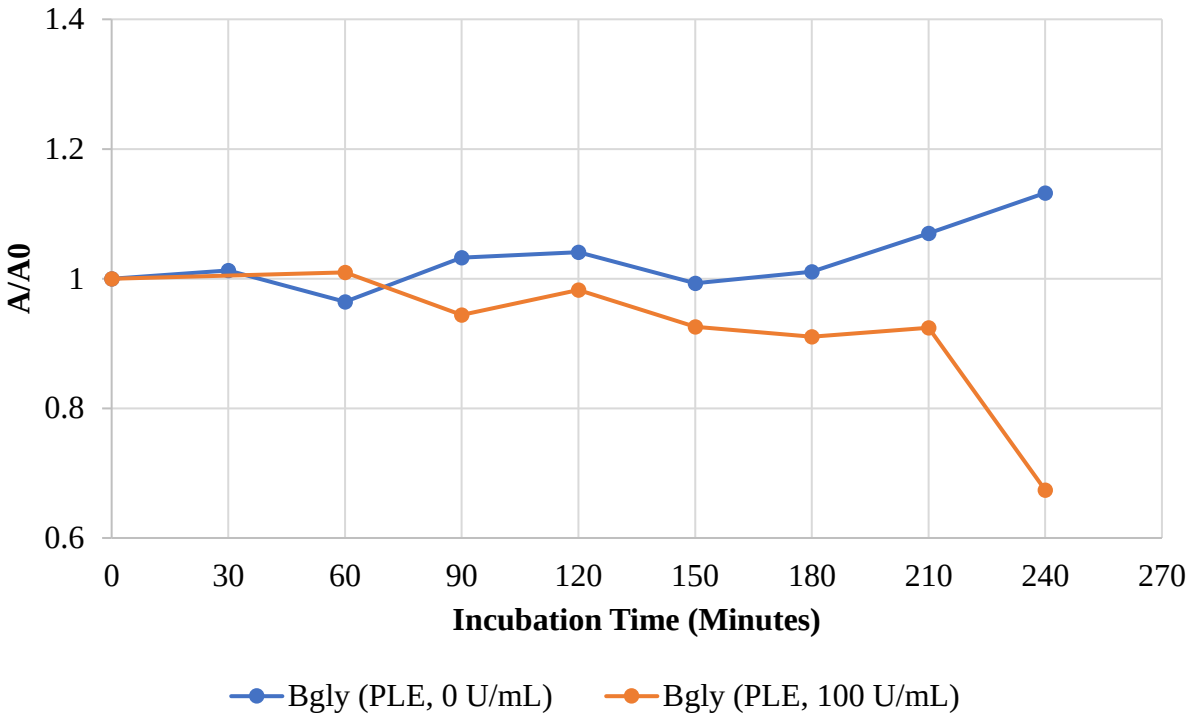

Figure 2.4. Stability of *N*-benzoyl glycine (Bgly) in pig liver esterase (PLE).

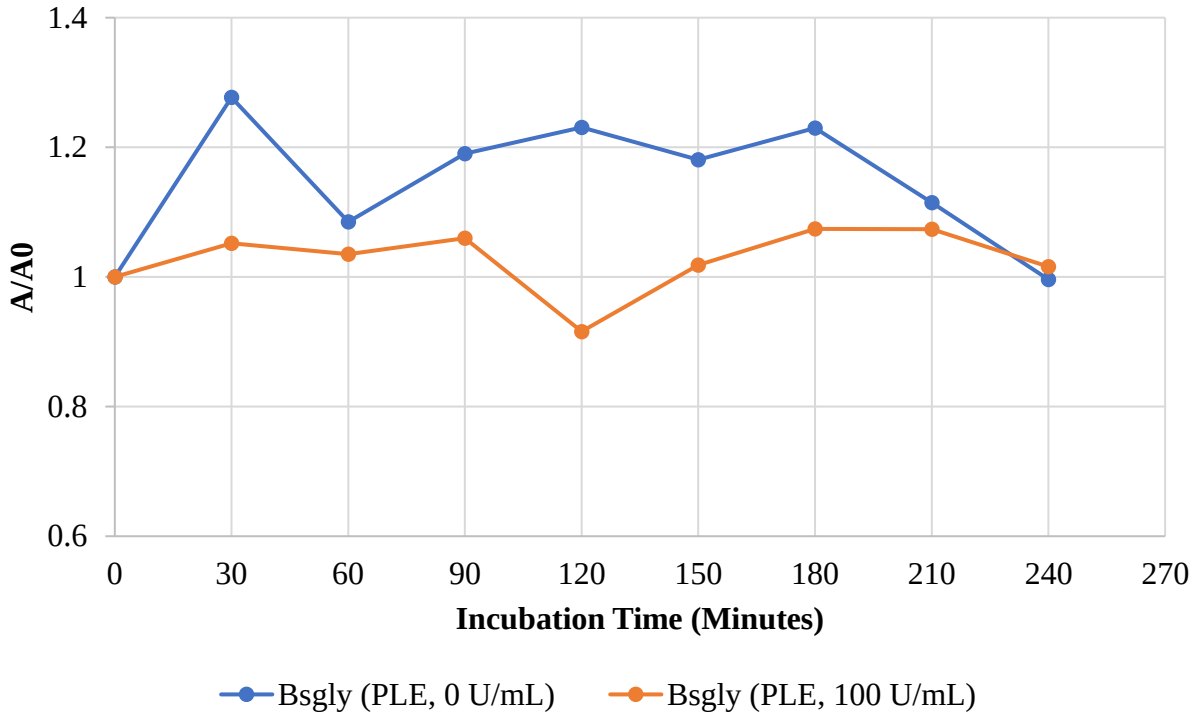

Figure 2.5. Stability of *N*-benzenesulfonyl glycine (Bsgly) in pig liver esterase (PLE).

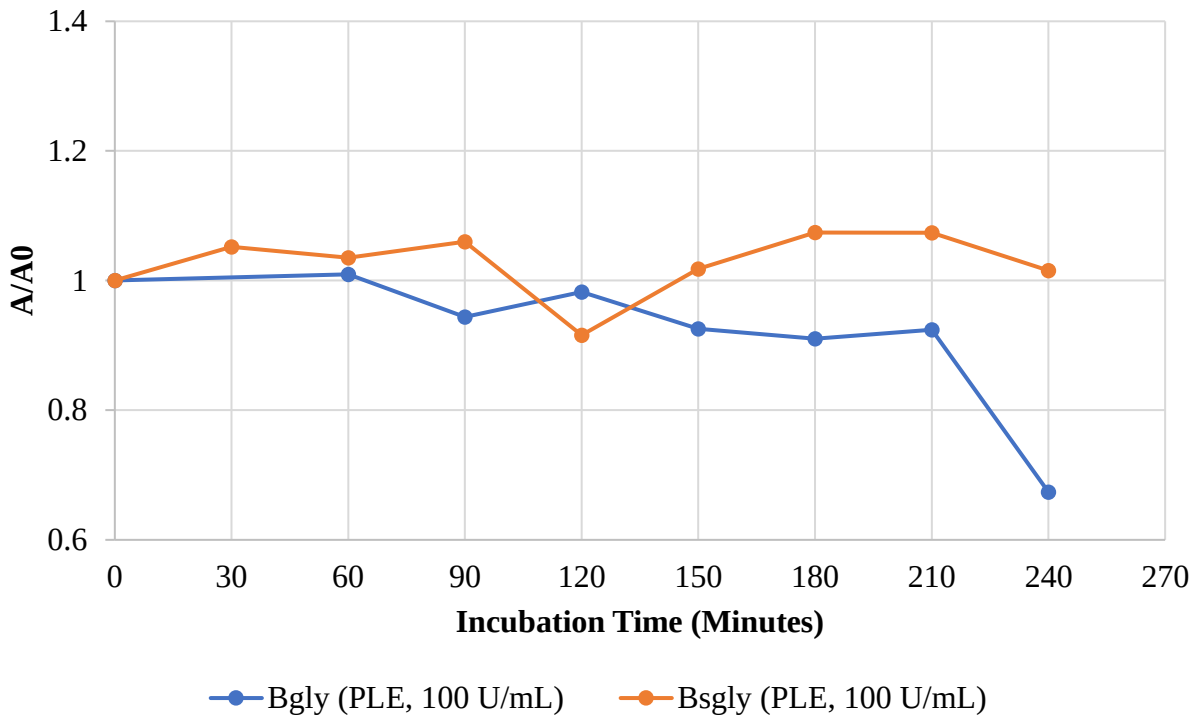

Figure 2.6. Stability of *N*-benzoyl glycine (Bgly) *vs N*-benzenesulfonyl glycine (Bsgly) in pig liver esterase (PLE).

The results show that *N*-benzoyl glycine (Bgly) *vs N*-benzenesulfonyl glycine are stable in 10 mM potassium phosphate buffer at pH 7.4 pH at 37 °C for at least 240 minutes. Additionally, both *N*-benzoyl glycine and *N*-benzenesulfonyl glycine remained stable when incubated with 100 U/mL PLE over 210 minutes. *N*-Benzoyl glycine, showed a decrease in concentration between 210 and 240 minutes, but it as we did not get to analyse replicates, it is unclear whether this is a true decrease or an outlier. The earlier TLC results did imply some glycine formation occurring for both reactions, which is inconsistent with these findings. It is possible that the ninhydrin positive peaks were not glycine but arising from PLE degradation. These HPLC stability results indicate that *N*-benzoyl glycine and *N*-benzenesulfonyl glycine are not highly susceptible to pig liver esterase or this class of enzyme in general. As these are very simple model systems, it may also be the case that once more sophisticated systems are employed with more complex peptides and labelling groups that they are more vulnerable to enzymatic degradation.

To verify the results seen in this study, the incubation studies will need to be repeated for *N*-benzoyl glycine and *N*-benzenesulfonyl glycine, with replicates. Control with the PLE (20, 50 or 100 U/mL) in the absence of the glycine derivatives will also be conducted. Additionally, the HPLC method will need to be optimised for analysis of these experiments. As seen in the representative HPLC spectra shown in Appendix 1, the HPLC method was not set up to allow monitoring of both the starting compounds (*N*-benzoyl glycine and *N*-benzenesulfonyl glycine) and their hydrolysis products

benzoic acid and benzenesulfonic acid, respectively, and it did not have a flat baseline, making analysis of the peak areas unreliable. Moving forward, a key step will be developing an optimised HPLC method with the HPLC system in-house at Macquarie University (once it is available again) for accurate analysis of the starting materials and aromatic products.

In a similar method to that described in this chapter, future metabolic stability studies will be performed where assay solutions of the target compounds are incubated with an enzyme or biological media, with aliquots taken at set time intervals, quenched, then analysed by either HPLC (PDA detection) or LC-MS. With replicates being performed for each sample and condition. There are many choices of enzyme and/or biological media for future assays.

The Cytochrome P450 family of enzymes are involved with the metabolic clearance of approximately 60% of marketed drugs from the body.[81] As a result, they are highly desirable for elucidating the extent and route of the metabolism of new compounds. Due to this, measuring the stability of the target compounds against recombinant cytochrome P450 enzymes would be valuable in future studies to further determine the stability of the sulfonamide compounds compared to the amide compounds. Performing a hepatocyte stability assay with the target compounds would also be highly advantageous, since while not as readily available as recombinant cytochrome P450 enzymes, hepatocytes contain the full complements of hepatic drug metabolising enzymes, for both phase I and II metabolism, including cytochrome P450 enzymes.[82] The incubation of new radiopharmaceuticals in human, mouse or rat plasma has also been demonstrated in the literature for testing the metabolic stability.[55,83,84]

2.3 Conclusions

N-Benzoyl glycine and *N*-benzenesulfonyl glycine were successfully synthesised. These model compounds were then used to test the metabolic stability of amides compared to sulfonamides against pig liver esterase. Both *N*-benzoyl glycine and *N*-benzenesulfonyl glycine were relatively stable for up to 240 minutes at 37 °C in a buffered system at physiological pH, including in the presence of pig liver esterase (100 U/mL). Future work will further test the metabolic stability of amide verses sulfonamide compounds by repeating these experiments and by exploring further stability studies with additional enzymes and biological media. This work will also utilise more sophisticated amide and sulfonamide systems.

CHAPTER THREE

Studies Towards Efficient Direct Labelling of Peptides with Fluorine-18

This chapter describes studies performed to synthesise a series of bifunctionalised compounds for future conjugation to peptides and subsequent radiofluorination. The work in this chapter was performed in parallel to the work described in Chapter 2.

3.1 Introduction

As described in Chapter 1, many strategies have been developed for the direct labelling of peptides with fluorine-18. The desire for direct labelling strategies is that they allow for the radiofluorination of peptides in a single time efficient step. This results in molar activities higher than those achieved with indirect labelling strategies. At the core of most direct labelling strategies is the synthesis of bifunctional compounds that are activated towards an initial peptide conjugation and a subsequent radiofluorination of the peptide conjugated system. **Figure 3.1** illustrates this direct labelling strategy with some of the most widely used bifunctional compounds, which conjugate to free amines on the target peptide.

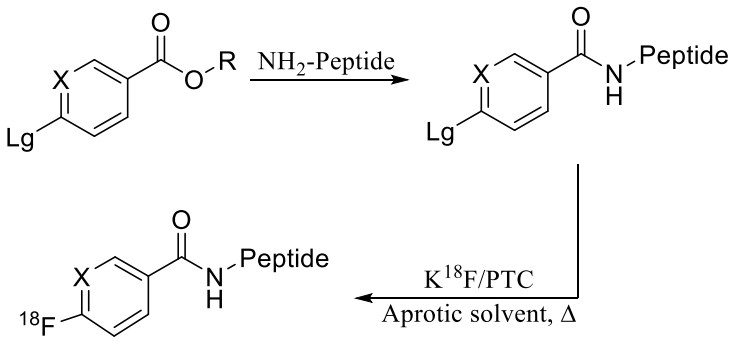

Lg = Good leaving group such as trimethylamine (triflate salt) or NO_2. X = Electron withdrawing moiety such as; C-CN, C-CF_3 or N. R = H or active ester. PTC = phase-transfer catalyst.

Figure 3.1. Generic scheme for direct labelling of peptides with fluorine-18.

The trimethylbenzenaminium (TMA) salts shown in **Figure 3.2** are particularly popular as they contain i) the benzoic acid moiety that can be converted into activated esters for facile peptide conjugation with free amines; ii) a trimethylamine group that is highly activated towards radiofluorination by nucleophilic aromatic substitution due especially to the presence of the electron withdrawing CN, CF_3 or pyridyl groups; and iii) the radiofluorinated product is typically readily purified from the starting material (TMA triflate salt) due to their very different polarities. While these TMA salts have been widely used in the literature, there have been no studies to directly compare all three compounds under the same conditions with the same peptide targets. This work

aimed to synthesise activated esters based on these three compounds, in preparation for their subsequent peptide conjugation and comparative fluorination studies.

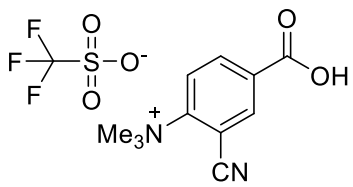

4-carboxy-2-cyano-*N*,*N*,*N*-trimethylbenzenaminium trifluoromethanesulfonate

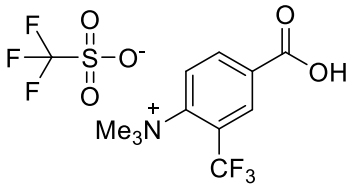

4-carboxy-*N*,*N*,*N*-trimethyl-2-(trifluoromethyl)benzenaminium trifluoromethanesulfonate

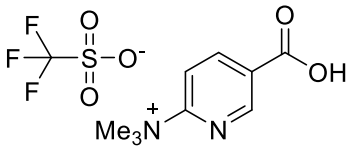

5-carboxy-*N*,*N*,*N*-trimethylpyridin-2-aminium trifluoromethanesulfonate

Figure 3.2. Target amide forming bifunctional compounds.

This work also aimed to synthesise the sulfonic acids shown in **Figure 3.3**, and their activated sulfonate esters, for subsequent peptide conjugation and fluorination studies. As described in Chapter 1, the sulfonamide analogues were of interest due to the potential benefit that the sulfonamide bond may offer over an amide bond in terms of metabolic stability. Additionally, there is a precedent in the literature showing the use of a sulfonamide as an activating group for nucleophilic aromatic substitution.[85] Thus, increased electron withdrawing effects offered by the sulfonamide bond over the amide bond may act to further activate the peptide conjugated system towards fluorination *via* nucleophilic aromatic substitution. There are also reports that show the distinctly different hydrogen-bonding and geometrical preferences between carboxamides and sulfonamides can lead to differences in peptide backbone folding if one is substituted for the other.[86] For example, the increased acidity of the sulfonamide NH compared to the carboxamide NH, allows it to better participate in hydrogen bonding events. Due to this, the potential impacts substituting a carboxamide for sulfonamide could make to both peptide stability and activity towards the target site, are worthy of investigation.

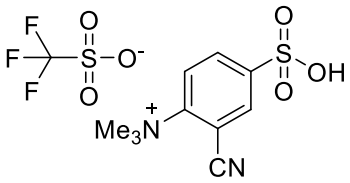

2-cyano-*N*,*N*,*N*-trimethyl-4-sulfobenzenaminium trifluoromethanesulfonate

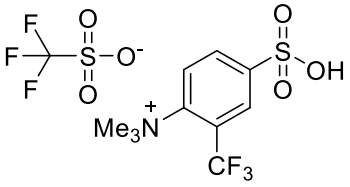

4-carboxy-*N*,*N*,*N*-trimethyl-2-(trifluoromethyl)benzenaminium trifluoromethanesulfonate

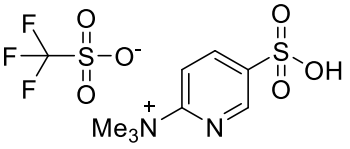

5-carboxy-*N*,*N*,*N*-trimethylpyridin-2-aminium trifluoromethanesulfonate

Figure 3.3. Target sulfonamide forming bifunctional compounds.

This chapter describes the work undertaken during the Master of Research project to trial the synthesis of some of the proposed bifunctional compounds.

3.2 Results and Discussion

3.2.1 Initial Synthesis Strategy

The use of activated esters on prosthetic groups for ease of peptide conjugation has been well documented for direct radiolabelling strategies.[51,87] Consequently, this work initially aimed to synthesise the compounds proposed in **Figure 3.2** and **Figure 3.3** with the addition of a *p*-nitrophenyl ester moiety to increase the ease of peptide conjugation. These target 4-nitrophenyl derivatives are shown in **Figure 3.4**.

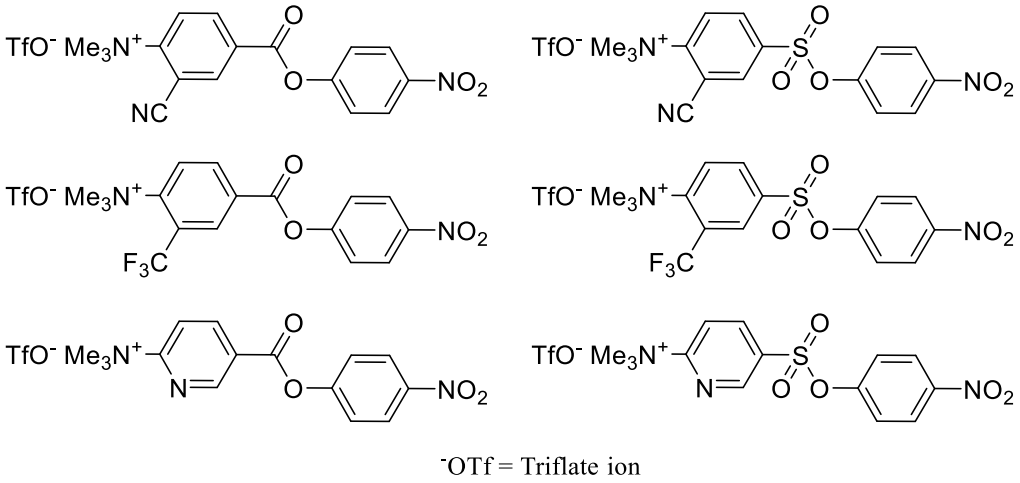

Figure 3.4. Target 4-nitrophenyl esters bearing the trimethylamine (triflate salt) moiety.

The 4-nitrophenyl moiety was chosen for the active esters as previous studies have used it to enhance prosthetic groups towards peptide conjugation[88] and the precursor 4-nitrophenol was readily available. An additional advantage of the 4-nitrophenol ester moiety is that there would be a clear colour change to show if the ester is hydrolysed.

This work aimed to make use of glycine ethyl ester as a simple model for a peptide while performing the initial trials to establish the best performing compounds in relation to ease of peptide conjugation and ease of the subsequent fluorination **Figure 3.5**. Glycine ethyl ester was chosen as the syntheses of the model compounds were anticipated to be very straightforward and it was readily available and vastly cheaper than representative peptides. Additionally, unlike use of glycine, as the protected ethyl ester, it allows for one of the potential sources for the protonation and thus deactivation of free nucleophilic fluorine during fluorination to be avoided. The glycine ethyl ester conjugated model would enable more trials testing ease of conjugation and fluorination to be performed in a cheap, efficient and timely manner when compared to other model systems. Thus, trends in conjugation and fluorination chemistry with the target compounds chosen (**Figure 3.4**) could more easily be elucidated before trialling the best performing compounds with more realistic peptide systems. The general method for the conjugation of the 4-nitrophenyl derivatives to glycine ethyl ester and

subsequent fluorination of the conjugated systems is shown in **Figure 3.5**. Cold ^{19}F fluorination was proposed for these model studies for obvious safety reasons, cost and convenience of conducting this work within the Macquarie University laboratory. Additionally, recent work by Zhang *et al.*[89] has shown that ^{18}F-syntheses can be readily optimised using fluorine-19.

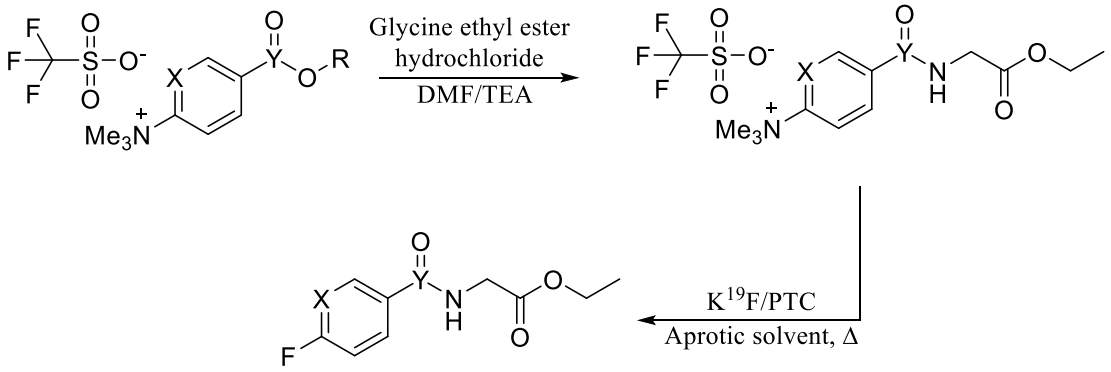

X = C-CN, C-CF_3 or N. Y = C or SO. R = 4-nitrophenyl. PTC = phase-transfer catalyst.

Figure 3.5. General scheme for the conjugation of the target 4-nitrophenyl derivatives to glycine ethyl ester and subsequent fluorination of the conjugated system with cold fluorine-19.

3.2.1.1 Synthesis of 4-Nitrophenyl Esters

The syntheses of the *p*-nitrophenyl esters (**5**, **7** and **9**) were proposed to be conducted from direct condensation of the carboxylic acids **(4)**, **(6)** and **(8)** with *p*-nitrophenol (**Scheme 3.1**).

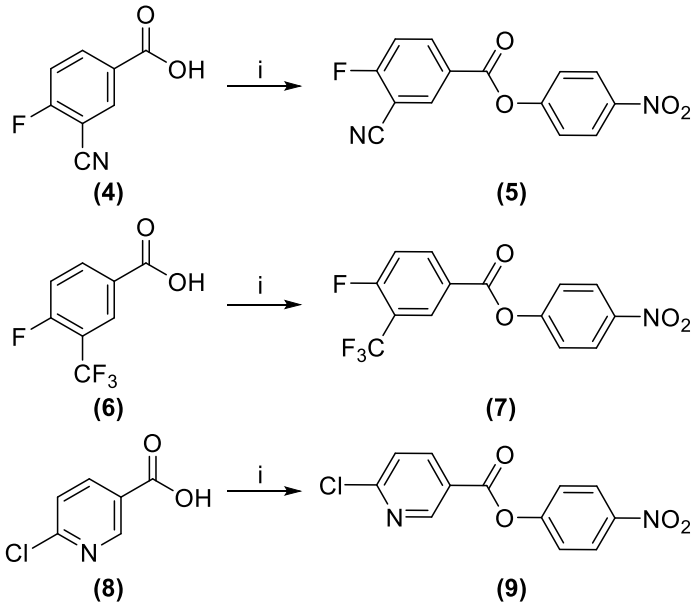

Reagents and conditions:
(i) 4-nitrophenol, *N,N'*-dicyclohexylcarbodiimide, dioxane, overnight.

Scheme 3.1. Synthesis of 4-nitrophenyl esters.

As carboxylic acid **(4)** was not commercially available, this was obtained by oxidation of the commercially available aldehyde, 3-cyano-4-fluorobenzaldehyde **(3)** (**Scheme 3.2**).[90]

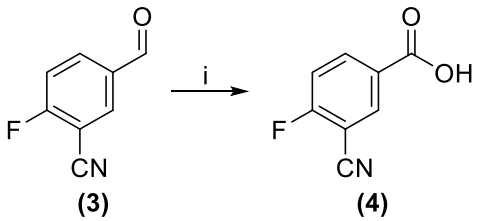

Reagents and conditions:
(i) KH_2PO_4, H_2O_2, $NaClO_2$, H_2O, Acetonitrile, 0 °C, 2 hours.

Scheme 3.2. Synthesis of 3-cyano-4-fluorobenzoic acid **(4)**.

The aldehyde **(3)** was readily oxidised using $NaClO_2/H_2O_2$ to afford 3-cyano-4-fluorobenzoic acid **(4)** in 87% yield, utilising the method of Woo *et al.*[90] ^{1}H NMR, EI-MS and melting point data were in agreement with the literature.[55,90]

The respective benzoic acids **(4)**, **(6)** and **(8)** were readily converted to their corresponding 4-nitrophenyl derivatives **(5)**, **(7)** and **(9)** utilising a method adapted from Olberg *et al.*[87] (**Scheme 3.1**), with 4-nitrophenol in the presence of *N,N'*-dicyclohexylcarbodiimide. This method gave an unoptimized yields of 61% for **(5)**, 63% for **(7)** and 61% for **(9)**. The melting points of **(5)** and **(7)** have not been reported, but the melting point of **(9)** was consistent with the literature.[91] The EI-MS data for each compound showed the respective $[M]^+$ peaks and the characteristic peak of $[M\text{-}OC_6H_4NO_2]^+$. The ^{1}H NMR data showed the appearance of a second aromatic ring for each product, in addition to characteristic aromatic H-H couplings for all compounds, and characteristic aromatic H-F couplings for compounds **(5)** and **(7)**.

The synthesis of the sulfonate analogue, 4-nitrophenyl 4-fluoro-3-cyanobenzene sulfonate **(12)**, was achieved in two steps starting from the commercially available amine, 5-amino-2-fluorobenzonitrile **(10)**, as shown in **Scheme 3.3**.[88,92]

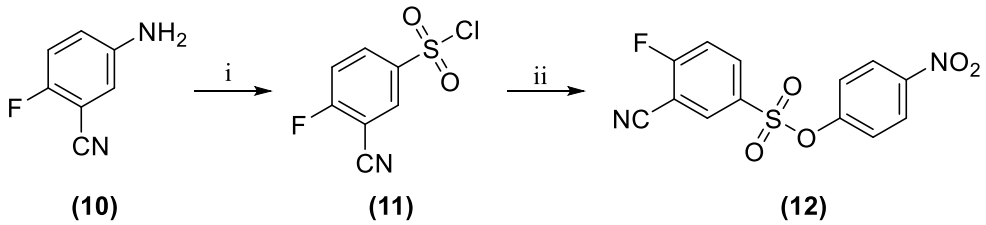

Reagents and conditions: (i) $SOCl_2$, CuCl, $NaNO_2$, H_2O, 0 °C, 1 hour;
(ii) 4-nitrophenol, trimethylamine, dioxane, 0 °C, 1 hour.

Scheme 3.3. Synthesis of 4-nitrophenyl 4-fluoro-3-cyanobenzene sulfonate **(5)**.

3-Cyano-4-fluorobenzenesulfonyl chloride **(11)** was synthesised from 5-amino-2-fluorobenzonitrile **(10)** *via* diazonium salt chemistry utilising the method of Grewal *et al.*[92] in 74% yield. The sulfonyl chloride **(11)** was converted to the *p*-nitrophenyl sulfonate **(12)** utilising a method adapted from Haskali *et al.*[88], with 4-nitrophenol in the presence of triethylamine. This method gave an unoptimised yield of 72%. EI-MS analysis of **(11)** showed characteristic mass peaks of $[M\text{-}Cl]^+$ and $[M\text{-}SO_2Cl]^+$, while analysis of **(12)** showed characteristic $[M]^+$ and $[M\text{-}SO_2C_6H_4NO_2]^+$ mass peaks. ^1H NMR of **(11)** showed loss of the NH_2 and analysis of **(12)** showed the appearance of a second aromatic ring (*para*-disubstituted). Both products also showed characteristic aromatic H-H and H-F couplings.

3.2.1.2 Addition of TMA Moiety to 4-Nitrophenyl Esters

The synthesis of the target compound, 2-cyano-*N*,*N*,*N*-trimethyl-4-((4-nitrophenoxy)carbonyl)benzenaminium trifluoromethanesulfonate **(14)** was anticipated to occur from the 4-nitrophenyl ester **(5)**, as shown in **Scheme 3.4**.[55,93]

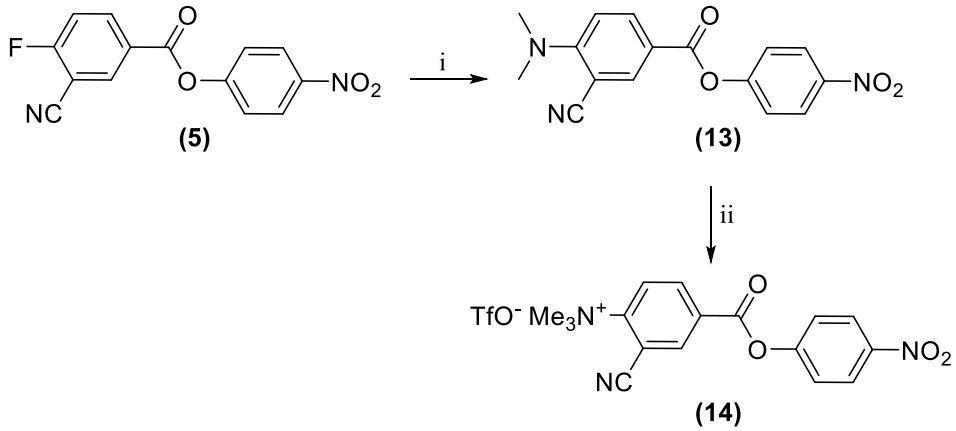

Reagents and conditions: (i) dimethylamine hydrochloride, K_2CO_3, DMSO, overnight; (ii) methyl trifluoromethanesulfonate, dry DCM, under argon, 24 hours.

Scheme 3.4. Planned synthesis of 2-cyano-*N*,*N*,*N*-trimethyl-4-((4-nitrophenoxy)carbonyl)benzenaminium trifluoromethanesulfonate **(14)**.

Substitution of the *para*-fluorine of the 4-nitrophenyl ester **(5)** with dimethylamine was attempted through the treatment of **(5)** with dimethylamine hydrochloride in the presence of potassium carbonate, using a method adapted from Becaud *et al.*[55] However, this was not successful as characterisation of the product by EI-MS identified it as a mixture of 3-cyano-4-(dimethylamino)-*N*,*N*-dimethylbenzamide (~69%) and 3-cyano-4-fluoro-*N*,*N*-dimethylbenzamide (~31%) (**Scheme 3.5**). The formation of these products is clearly a result of the *p*-nitrophenyl ester being too reactive and consequently being attacked by the dimethylamine in preference to the *para*-fluorine.

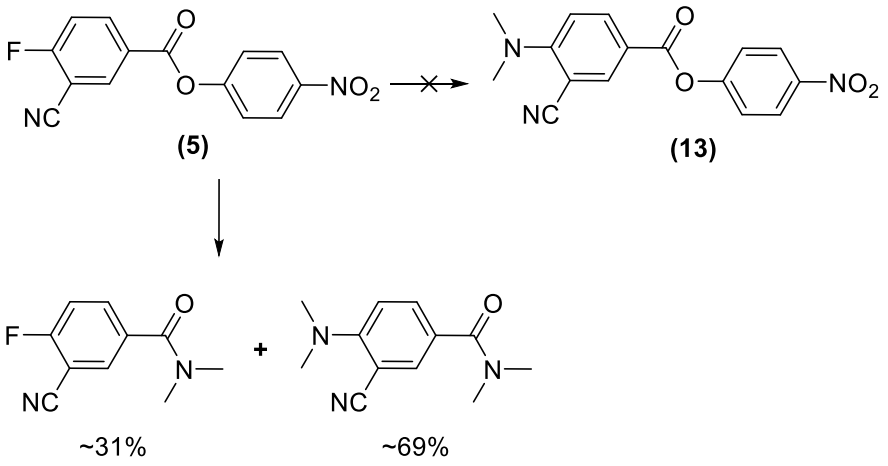

Scheme 3.5. Attempted synthesis of 4-nitrophenyl-4-(dimethylamino)-3-cyanobenzoate **(13)**.

The failure of this reaction to give any of the desired compound **(13)**, was unfortunate. In work by Olberg *et al.*, the TMA salt, *N,N,N*-trimethyl-5-((2,3,5,6-tetrafluorophenoxy)-carbonyl)pyridine-2-aminium trifluoromethanesulfonate has been directly produced from a 2,3,5,6-tetrafluorophenyl active ester precursor through treatment with trimethylamine in tetrahydrofuran (**Figure 3.6**).[87]

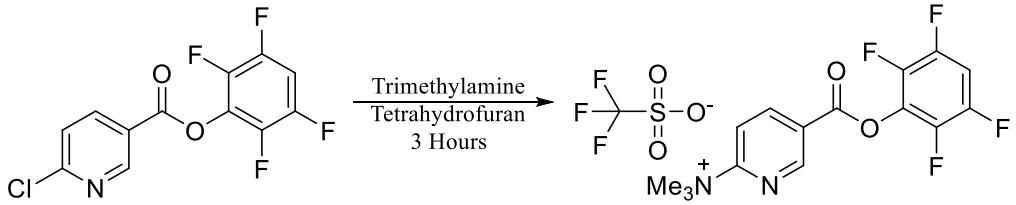

Figure 3.6. Synthesis of *N,N,N*-trimethyl-5-((2,3,5,6-tetrafluorophenoxy)-carbonyl)pyridine-2-aminium trifluoromethanesulfonate by Olberg *et al.*[87]

Olberg *et al.*, however, found that attempts to synthesise the *N*-hydroxysuccinimide ester analogue were unsuccessful, as extensive decomposition of the ester occurred on contact with trimethylamine.[87] This suggests that the choice of active ester moiety is critical for such reactions. Due to this, it may be worth revisiting the addition of an active ester moiety to the target compounds in future studies, testing a range of other active esters such as *N*-hydroxysuccimide, *N*-hydroxybenzotriazole or 2,3,5,6-tetrafluorophenyl.[87,88] Due to limited time this was not pursued within this Master of Research project.

3.2.2 Second Synthesis Strategy

Due to the lack of success of being able to form the TMA salt of the *p*-nitrophenyl ester **(14)**, a new approach using methyl esters, based on work by Becaud *et al.*,[55] was planned to examine the relative ease of fluorination of the different activated aromatic systems (**Figure 3.2** and **Figure 3.3**). The structures of the new target molecules are shown in **Figure 3.7**.

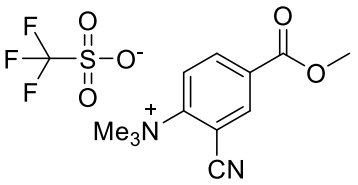

2-cyano-4-(methoxycarbonyl)-*N*,*N*,*N*-trimethylbenzenaminium trifluoromethanesulfonate

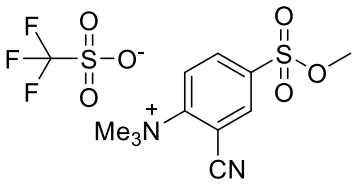

2-cyano-4-(methoxysulfonyl)-*N*,*N*,*N*-trimethylbenzenaminium trifluoromethanesulfonate

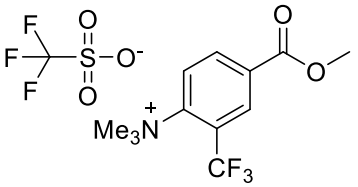

4-(methoxycarbonyl)-*N*,*N*,*N*-trimethyl-2-(trifluoromethyl)benzenaminium trifluoromethanesulfonate

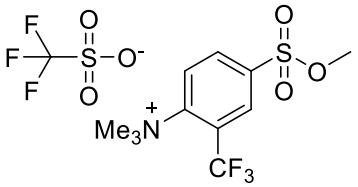

4-(methoxysulfonyl)-*N*,*N*,*N*-trimethyl-2-(trifluoromethyl)benzenaminium trifluoromethanesulfonate

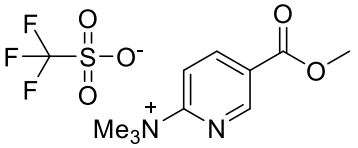

5-(methoxycarbonyl)-*N*,*N*,*N*-trimethylpyridin-2-aminium trifluoromethanesulfonate

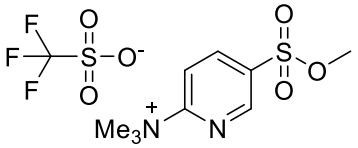

5-(methoxysulfonyl)-*N*,*N*,*N*-trimethylpyridin-2-aminium trifluoromethanesulfonate

Figure 3.7. Target methyl ester compounds.

3.2.2.1 Synthesis of Methyl Ester Derivatives with the TMA Moiety

Utilising a method adapted from Becaud *et al.*[55], 4-(methoxycarbonyl)-*N*,*N*,*N*-trimethyl-2-(trifluoromethyl) benzenaminium trifluoromethanesulfonate **(18)** was achieved in 3 steps starting from commercially available, 4-fluoro-3-(trifluoromethyl)benzoic acid **(15)** (**Scheme 3.6**).[55]

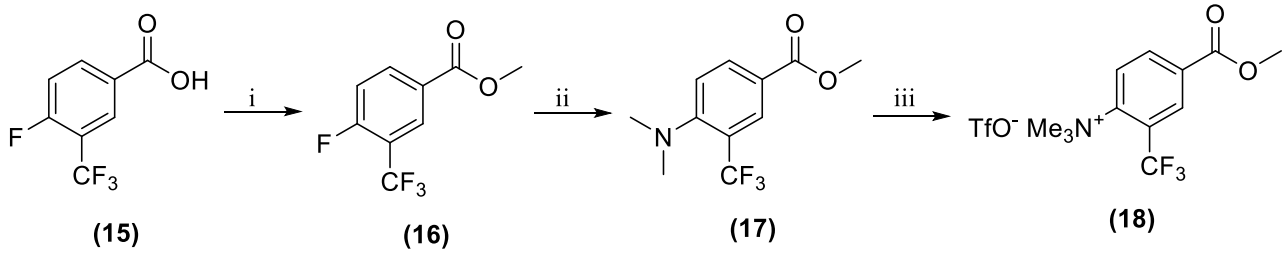

(15) **(16)** **(17)** **(18)**

Reagents and conditions: (i) CH_3COCl, methanol, 24 hours;
(ii) dimethylamine hydrochloride, K_2CO_3, DMSO, 48 hours;
(iii) methyl trifluoromethanesulfonate, dry DCM, under argon, 70 hours.

Scheme 3.6. Synthesis of 4-(methoxycarbonyl)-*N*,*N*,*N*-trimethyl-2-(trifluoromethyl) benzenaminium trifluoromethanesulfonate **(18)**.

Methyl 4-fluoro-3-(trifluoromethyl)benzoate **(16)** was synthesised in a 59% yield, through the esterification of **(15)** with methanol in the presence of acetyl chloride. Dimethylamination of the methyl ester **(16)** to give methyl 4-(dimethylamino)-3-(trifluoromethyl)benzoate **(17)** was achieved

with a yield of 74%, through the treatment of **(16)** with dimethylamine hydrochloride in the presence of potassium carbonate. The synthesis of 4-(methoxycarbonyl)-*N*,*N*,*N*-trimethyl-2-(trifluoromethyl) benzenaminium trifluoromethanesulfonate **(18)** was achieved in an unoptimised yield of 3%, from the methylation of **(17)** with methyl trifluoromethanesulfonate in dry dichloromethane in a sealed inert atmosphere of argon. ^{1}H NMR and EI-MS of **(16)** showed the characteristic appearance of a methyl ester group and characteristic $[M]^{+}$ and $[M\text{-}OCH_3]^{+}$ mass peaks. ^{1}H NMR and EI-MS of **(17)** and ^{1}H NMR of **(18)** were in agreement with the literature.[55] Unfortunately, **(18)** could not be characterised by mass spectrometry since Macquarie University's in-house LC-MS facilities were rendered unavailable during the time of this work. While the achieved yield for **(18)** was low, the literature yield was only 32%.[55]

Utilising a method based on Becaud *et al.*[55], the synthesis of 5-(methoxycarbonyl)-*N*,*N*,*N*-trimethylpyridin-2-aminium trifluoromethanesulfonate **(22)** was planned through a three step procedure starting from commercially available 6-chloronicotinic acid **(19)** (**Scheme 3.7**).[55]

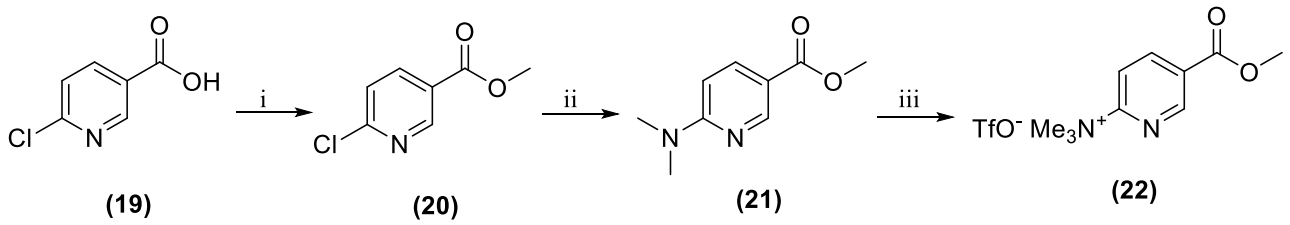

(19) **(20)** **(21)** **(22)**

Reagents and conditions: (i) CH_3COCl, methanol, 24 hours;
(ii) dimethylamine hydrochloride, K_2CO_3, DMSO, 48 hours;
(iii) methyl trifluoromethanesulfonate, dry DCM, under argon, 24 hours.

Scheme 3.7. Planned synthesis of 5-(methoxycarbonyl)-*N*,*N*,*N*-trimethylpyridin-2-aminium trifluoromethanesulfonate **(22)**

The synthesis of methyl 6-chloronicotinate **(20)** was attempted through the esterification of 6-chloronicotinic acid with methanol in the presence of acetyl chloride. However, characterisation of the product by ^{1}H NMR and EI-MS identified it to be a mixture of the desired product **(20)** (~81%) and methyl 6-methoxynicotinate (~19%) (**Scheme 3.8**).

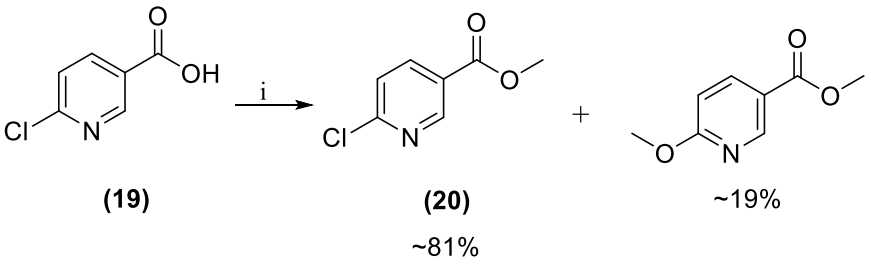

Reagents and conditions: (i) CH_3COCl, methanol, 24 hours.

Scheme 3.8. Attempted synthesis of methyl 6-chloronicotinate **(20).**

The majority of the mass of the product mixture was the desired product **(20)** however due to limited time in the Masters of research project there was not enough time to trial purification methods.

3.3 Conclusions

The purpose of the work in this chapter was to trial the initial steps required to determine which of the target activated systems (**Figure 3.2** and **Figure 3.3**) are the most activated towards peptide conjugation and fluorination. This was initially attempted *via* the synthesis of 4-nitrophenyl active ester derivatives (**Figure 3.4**). However, it was found that the 4-nitrophenyl ester moiety was too activated. Due to the time constraints of the Masters of research project, a different method was pursued based upon work by Becaud *et al.*,[55] which involved the synthesis of TMA bearing methyl ester derivatives (**Figure 3.7**). It was anticipated that these could be used to determine the best target system for rapid fluorination, prior to further peptide conjugation studies. To this end, synthesis of a TMA bearing methyl ester derivative, 4-(methoxycarbonyl)-*N*,*N*,*N*-trimethyl-2-(trifluoromethyl) benzenaminium trifluoromethanesulfonate **(18)** was successfully trialled, with an unoptimised yield of 3%.

Moving forward, future work will aim to synthesise all target TMA bearing methyl ester derivatives (**Figure 3.7**) with optimised yields such that they can be synthesised in sufficient quantities to pursue fluorination studies to determine which of the compounds show the best activity towards fluorination. The design of these fluorination studies will be based upon the methods of Becaud *et al.*[55] and Zhang *et al*.[94], and will involve fluorination of the target TMA bearing methyl ester derivatives with fluorine-19 under a battery of different reaction conditions. This will then help inform the best aromatic scaffolds for future direct fluorination of the glycine ethyl ester and finally peptide conjugates relevant to PET.

CHAPTER FOUR

Materials and Methods

4.1 General

All starting materials, reagents and solvents were purchased from Sigma-Aldrich (USA) and used without further purification, unless otherwise stated. Pig liver esterase was purchased from Sigma Aldrich (USA; pig liver esterase, PLE; Sigma E3019-3.5 kU, Batch# SLBM5398V, 18 U/mg). All water used was purified by reverse osmosis. Argon (99.9999%) and Helium (99.9999%) were purchased from BOC (Australia). Nitrogen gas was provided by liquid nitrogen boil-off available on-tap in the laboratory at Macquarie University.

Normal-phase TLC studies were performed using Merck silica gel 60 F_{254} aluminium TLC plates (Merck, USA). Reversed phase TLC studies were performed using Merck TLC Silica gel 60 RP-18 $F_{254}S$ aluminium TLC plates (Merck USA). TLC plates were visualised under UV light (254 nm) and by ninhydrin spray (0.2% in butanol + 5% acetic acid).

Melting points were obtained on a Stuart (UK) SMP10 melting point apparatus. They were uncorrected.

All preparative column chromatography was carried out using Kieselgel 60 (0.040-0.063 mm) silica gel (Merck, USA) with solvent mixes as specified within the individual experimental methods.

The removal of solvent *in vacuo* was performed on a rotary evaporator under vacuum at 45 °C. Further drying was performed on a high vacuum system at room temperature.

400 MHz NMR studies were performed on a Bruker Ascend™ 400 NMR equipped with a Bruker SampleXpress autosampler. The NMR was controlled by a standard desktop PC running Bruker IconNMR software (Version 5.0.6, Build 32). All NMR spectra were processed with Bruker TopSpin software (Version 3.5, pl 7). ^{1}H-NMR spectra were recorded as δ values relative to the solvent signal. Coupling constants are reported in Hertz. The multiplicity is defined by s (singlet), d (doublet), t (triplet), br (broad), m (multiplet).

UV-Vis studies were performed using a Jasco (V-760) UV-Vis spectrophotometer fitted with a Jasco (PAC-743R) Peltier cell changer (Jasco Corporation, Japan) and quartz cuvettes (1 cm pathlength). The spectrometer was controlled by a standard desktop PC running Jasco Spectra Manager software (version 2. 14.02, Build 3).

A Shimadzu GC-MS system (Shimadzu Corporation, Japan) was used for electron impact mass spectrometry (EI-MS) analysis. The GC-MS system consisted of a Shimadzu auto sampler (AOC-20s), Shimadzu auto injector (AOC-20i), Shimadzu gas chromatograph (GC-2010) equipped with a split/split-less injector, and a Shimadzu gas chromatograph mass spectrometer (GCMS-QP2010). The GC-MS was equipped with a Rtx®-5Sil MS column (Restek, USA), 30 m, 0.25 mm ID, 0.25 µm df. The GC-MS system was controlled by a standard desktop PC running Shimadzu LabSolutions GCMSsolution software (Version 2.72).

LC-MS for compounds incompatible with GC-MS was initially planned to be done in-house at Macquarie University, however, due to unforeseen circumstances, the instrument was rendered unavailable during the time it was required for this work. Similarly, analytical HPLC facilities at Macquarie University were also unavailable during the times it was required for this research.

Analytical HPLC methods for the analysis of samples from the stability assays were performed at the Australian Nuclear Science and Technology Organisation (ANSTO) by Dr Lidia Matesic using Waters HPLC equipment comprising: Waters 626 pump, In-line degasser AF, 600S Controller, 2996 Photodiode Array Detector, 717plus Autosampler and Empower 3 software. Samples were injected onto a Grace Alltima C18 53 mm × 7 mm, 3 µm analytical column.

4.2 Methods

4.2.1 Testing enzyme activity

To examine the activity of the pig liver esterase (PLE) purchased from Sigma Aldrich, a method adapted from Landowski *et al.*[77] was used in which PLE was assessed by a spectrometric assay using *p*-nitrophenyl butyrate, and monitored for the formation of *p*-nitrophenol spectrophotometrically at a wavelength of 405 nm.

Stock solutions of *p*-nitrophenyl butyrate (100 and 10 mM) were prepared in DMSO and used to prepare a series of assay solutions composed of *p*-nitrophenyl butyrate at final concentrations of 0.025 to 1 mM, in an assay medium of aqueous 10 mM potassium phosphate pH 7.4 containing 5% DMSO. The reaction was then started by adding 100 µL of freshly prepared PLE stock solution (28 µg/mL in aqueous 10 mM potassium phosphate pH 7.4) to each cuvette (pre-tempered to 37 °C). The formation of *p*-nitrophenol was then detected at 405 nm over 5 minutes at 37 °C. The preparation of these assay solutions is summarised in **Table 4.1**.

Table 4.1. Preparation of *p*-nitrophenyl butyrate (pNPB) assay solutions.

Final [pNPB] (mM)	Volume of pNPB stock added (µL)	Volume of DMSO added (µL)	Volume of 10 mM potassium phosphate pH 7.4 added (µL)	Volume of PLE stock added (µL)	Total volume (µl)
0.025	5[a]	95	1800	100	2000
0.05	10[a]	90	1800	100	2000
0.1	20[a]	80	1800	100	2000
0.2	4[b]	96	1800	100	2000
0.4	8[b]	92	1800	100	2000
0.8	16[b]	84	1800	100	2000
1.0	20[b]	80	1800	100	2000

[a]10 mM Stock solution; [b]100 mM stock solution. pNPB = *para*-nitrophenyl butyrate

GraphPad Prism 7, version 7.04 (GraphPad Software Inc., San Diego, CA), was used to fit the experimental data to the Michaelis-Menten equation (1).

$$v = \frac{V_{max} \cdot [S]}{K_m + [S]} \quad (1)$$

4.2.2 Testing Enzymatic Degradation of Amide *vs* Sulfonamide Compounds

To examine the stability of *N*-benzoyl glycine and *N*-benzenesulfonyl glycine in PLE, a method adapted from the work of Löser *et al*.[69] and Vine *et al*.[78] was used. For this method Stock solutions of *N*-benzoyl glycine and *N*-benzenesulfonyl glycine (100 mM each) were prepared in 10 mM potassium phosphate pH 7.4. The stability assays were started by adding freshly prepared PLE solution (1500 U/mL in aqueous 10 mM potassium phosphate buffer pH 7.4) at various volumes (final concentration 0, 20, 50 or 100 U/mL) to *N*-benzoyl glycine or *N*-benzenesulfonyl glycine solutions (final concentrations 1 mM in aqueous 10 mM potassium phosphate buffer pH 7.4) prepared from the stock solutions, and pre-tempered to 37 °C. The assay solutions were then incubated at 37 °C for 240 minutes.

After the addition of PLE, aliquots of 50 µL were withdrawn every 30 minutes up to a total time of 240 minutes. An additional aliquot (time 0) was taken immediately after the addition of PLE (or phosphate buffer in the case of the controls). Each aliquot was immediately quenched with 50 µL of a TFA solution (2% in acetonitrile), such that the quenched samples were 1% in TFA (*v/v*).

4.2.2.1 Analysis by TLC

The quenched samples were initially analysed by reversed phase TLC (eluent: 1:1:0.001 H_2O:CH_3CN:TFA), and normal-phase TLC (eluent: 1:0.001 EtOAc:TFA), with visualisation at 254 nm. The plates were then stained with a ninhydrin solution to visualise glycine.

4.2.2.2 Analysis by HPLC

Analysis of the stability assay samples was performed under contract at the Australian Nuclear Science and Technology Organisation (ANSTO) by Dr Lidia Matesic due to the unavailability of instrumentation at Macquarie University. To minimise cost of the analysis by a commercial third-party, only *N*-benzoyl glycine or *N*-benzenesulfonyl glycine incubation samples with the highest PLE concentration (100 U/mL) and the controls (0 U/mL) were chosen for analysis. For the analysis, 50 µL of each sample was diluted with 1000 µL of acetonitrile, then 30 µL of the resulting diluted sample was injected onto the HPLC system, under the gradient method shown in **Table 4.2**. With measurements recorded at 225 nm

Table 4.2. Gradient HPLC conditions used for the analysis of stability study samples.

Time (min)	Flow (mL/min)	CH_3CN + 0.1% TFA (%)	water + 0.1% TFA (%)
0.00	0.8	10	90
1.00	1.5	10	90
8.50	1.5	90	10
9.50	1.5	90	10
10.00	1.5	10	90
14.90	1.5	10	90
14.99	0.1	10	90

The data from this analysis is expressed as relative peak area (A/A_0) *vs* time (where A = peak area of the sample and A_0 = peak area of the sample at time zero).

4.3 Syntheses

4.3.1 *N*-Benzoyl glycine (1)

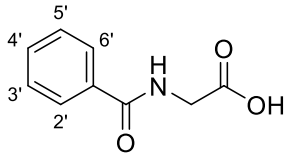

Glycine (1.51 g, 20.1 mmol) and NaOH (3.24 g, 81.1 mmol) were dissolved in water/acetonitrile (75/25%, 6 mL). The colourless solution was then cooled to 0 °C, and benzoyl chloride (2.44 mL, 21.0 mmol) was added dropwise to the stirred solution. Once the addition was complete, the red solution was stirred for two hours at 0 °C, then allowed to warm to room temperature and stirred for

an additional hour. The acetonitrile was removed *in vacuo*. The yellow aqueous solution was then acidified to pH 2 with concentrated aqueous HCl (36%) to cause precipitation. The white suspension was then vacuum filtered, and the filter cake was washed with water (5 mL) followed by ice-cold diethyl ether (5 mL). This afforded *N*-benzoyl glycine (1.84 g, 49%) as a white solid. Melting point: 189-190 °C (lit. 188-191 °C)[75].

^{1}H NMR (400 MHz, DMSO-d_6): δ (ppm) = 3.92 (d, *J* = 6.0 Hz, 2H, CH_2), 7.48 (dd, *J* = 7.3, 1.7 Hz, 2H, H-2', H-6'), 7.55 (tt, *J* = 7.3, 1.7 Hz, 1H, H-4'), 7.87 (m, 2H, H-3', H-5'), 8.83 (t, *J* = 6.0 Hz, 1H, NH), 12.60 (br s, 1H, OH). Spectral data were in agreement with the literature.[74]

4.3.2 *N*-Benzenesulfonyl glycine (2)

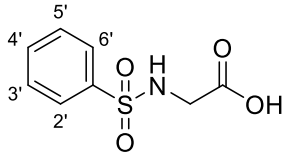

Benzenesulfonyl chloride (1000 µL, 7.84 mmol) was added dropwise over 30 minutes to a 70 °C stirred solution of glycine (603 mg, 8.04 mmol) and NaOH (330 mg, 8.25 mmol) in 15 mL of water. Once the addition was complete, the colourless solution was stirred for an additional two hours at 70 °C. The colourless solution was then cooled in an ice bath and acidified to pH 1 with concentrated aqueous HCl (36%) and vacuum filtered. The filtrate was extracted with diethyl ether (4 × 15 mL). The combined organic extracts were then washed with saturated aqueous brine (15 mL), dried over Na_2SO_4, gravity filtered, and the solvent was removed *in vacuo*. This afforded *N*-benzenesulfonyl glycine (228 mg, 13%) as a white powder. Melting point: 166-167 °C (lit. 165-166 °C)[76].

^{1}H NMR (400 MHz, DMSO-d_6): δ (ppm) = 3.58 (d, *J* = 6.0 Hz, 2H, CH_2), 7.56 (d, *J* = ~8 Hz, 2H, H-2', H-6'), 7.63 (tt, *J* = 7.3, 1.8 Hz, 1H, H-4'), 7.80 (d, *J* = ~8 Hz, 2H, H-3', H-5'), 8.04 (t, *J* = 6.1 Hz, 1H, NH), 12.68 (br s, 1H, OH).

4.3.3 3-Cyano-4-fluorobenzoic acid (4)

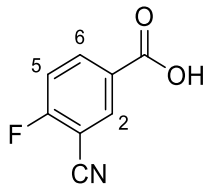

A solution of KH_2PO_4 (135 mg in 1.4 mL of H_2O) and aqueous H_2O_2 (30%, 180 µL) was added to a solution of 3-cyano-4-fluorobenzaldehyde (0.250 mg, 1.69 mmol) in acetonitrile (2.8 mL). The solution was cooled to 0 °C, then an aqueous solution of $NaClO_2$ (1.3 M, 2.8 mL) was slowly added with vigorous stirring. Stirring was continued at 0°C for two hours, at which point an aqueous solution

of Na_2SO_3 (180 mg in 550 µL of water) was added and the suspension stirred for an additional hour. 2 M aqueous HCl (2.8 mL) was then added and the yellow solution extracted with EtOAc (5 × 2.8 mL). The combined organic fractions were washed with water (2.8 mL) followed by saturated aqueous brine (2.8 mL), dried over Na_2SO_4, gravity filtered, and the solvent removed *in vacuo*. This afforded 3-cyano-4-fluorobenzoic acid (244 mg, 87%) as a cream powder. Melting point: 188-189 °C (lit. 187-188 °C)[90].

^{1}H NMR (400 MHz, $CDCl_3$): δ (ppm) = 7.33 (dd, *J* = 8.8, 8.8 Hz, 1H, H-5), 8.34 (ddd, *J* = 8.8, 5.1, 2.2 Hz, 1H, H-6), 8.39 (dd, *J* = 6.1, 2.2 Hz, 1H, H-2). EI-MS *m/z* (rel. intensity): 165 (47, $[M]^+$), 148 (100 $[M\text{-}OH]^+$), 120 (85 $[M\text{-}CO_2H]^+$). Spectral data were in agreement with the literature.[90]

4.3.4 4-Nitrophenyl 4-fluoro-3-cyanobenzoate (5)

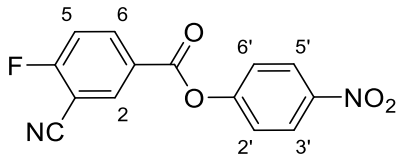

A solution of 3-cyano-4-fluorobenzoic acid **(4)** (607 mg, 3.68 mmol), 4-nitrophenol (512 mg, 3.68 mmol) and *N,N*'-dicyclohexylcarbodiimide (761 mg, 3.69 mmol) in dioxane (20 mL) was stirred overnight at room temperature. The resulting yellow suspension was vacuum filtered, and the filtrate concentrated *in vacuo*. The crude residue was subjected to silica gel chromatography (eluent: 100% DCM) to afford 4-nitrophenyl 4-fluoro-3-cyanobenzoate (642 mg, 61%) as a white powder. Melting point: 172-173 °C.

^{1}H NMR (400 MHz, $CDCl_3$): δ (ppm) = 7.66 (d, *J* = 9.2 Hz, 2H, H-2', H-6'), 7.79 (dd, *J* = 8.8, 8.8 Hz, 1H, H-5), 8.38 (d, *J* = 9.2 Hz, 2H, H-3', H-5'), 8.52 (ddd, *J* = 8.8, 5.0, 2.2 Hz, 1H, H-6), 8.74 (dd, *J* = 6.0, 2.2 Hz, 1H, H-2). EI-MS *m/z* (rel. intensity): 286 (0.52 $[M]^+$), 148 (100 $[M\text{-}OC_6H_4NO_2]^+$).

4.3.5 4-Nitrophenyl 4-fluoro-3-(trifluoromethyl)benzoate (7)

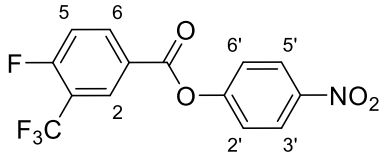

A solution of 4-fluoro-3-(trifluoromethyl)benzoic acid (0.606 g, 2.91 mmol), *p*-nitrophenol (0.408 g, 2.93 mmol) and *N,N*'-dicyclohexylcarbodiimide (0.607 g, 2.94 mmol) in dioxane (20 mL) was stirred overnight at room temperature. The resulting white suspension was vacuum filtered, and the filtrate dried *in vacuo*. The crude residue was subjected to silica gel chromatography (eluent: 100% DCM)

to afford 4-nitrophenyl 4-fluoro-3-(trifluoromethyl)benzoate (611 mg, 63%) as a white powder. Melting point: 92-93 °C.

^{1}H NMR (400 MHz, $CDCl_3$): δ (ppm) = 7.39 (dd, *J* = 9.2, 9.2 Hz, 1H, H-5), 7.43 (d, *J* = 9.2 Hz, 2H, H-2', H-6'), 8.35 (d, *J* = 9.2 Hz, 2H, H-3', H-5'), 8.42 (ddd, *J* = 9.2, 4.6, 2.1 Hz, 1H, H-6), 8.49 (dd, *J* = 6.7, 2.1 Hz, 1H, H-2). EI-MS *m/z* (rel. intensity): 329 (0.23 $[M]^+$), 191 (100 $[M\text{-}OC_6H_4NO_2]^+$).

4.3.6 4-Nitrophenyl 6-chloronicotinate (9)

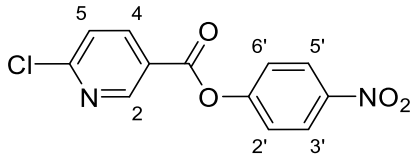

A solution of 6-chloronicotinic acid (602 mg, 3.82 mmol), 4-nitrophenol (531 mg, 3.82 mmol) and *N,N'*-dicyclohexylcarbodiimide (785 mg, 3.81 mmol) in dioxane (20 mL) was stirred overnight at room temperature. The resulting yellow suspension was then vacuum filtered, and the filtrate dried *in vacuo*. The crude residue was subjected to silica gel chromatography (eluent: 100% DCM). This afforded 4-nitrophenyl 6-chloronicotinate (651 mg, 61%) as a white powder. Melting point: 175-176 °C (lit. 172-173 °C).[91]

^{1}H NMR (400 MHz, $CDCl_3$): δ (ppm) = 7.44 (d, *J* = 9.1 Hz, 2H, H-2', H-6'), 7.53 (d, *J* = 8.4 Hz, 1H, H-5), 8.35 (d, *J* = 9.1 Hz, 2H, H-3', H-5'), 8.39 (dd, *J* = 8.4, 2.4 Hz, 1H, H-4), 9.17 (d, *J* = 2.4 Hz, 1H, H-2). EI-MS *m/z* (rel. intensity): 278 (0.70 $[M]^+$), 140 (100 $[M\text{-}OC_6H_4NO_2]^+$).

4.3.7 3-Cyano-4-fluorobenzenesulfonyl chloride (11)

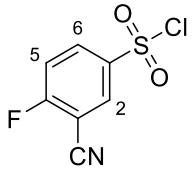

Water (10 mL) was cooled to 0 °C and thionyl chloride (2.0 mL, 25 mmol) was then added dropwise over 20 minutes. Once the addition was complete the clear solution was allowed to slowly warm to room temperature overnight. CuCl (23 mg, 0.23 mmol) was then added and the yellow solution was cooled to 0 °C. 5-Amino-2-fluorobenzonitrile (506 mg, 3.72 mmol) and conc. HCl (6 mL, 36%) were mixed and cooled to 0 °C. A solution of sodium nitrite (0.451 g, 6.53 mmol) in H_2O (5 mL) was then added drop wise to this solution over 15 minutes and stirred for an additional 15 minutes. This light brown solution was then added dropwise to the thionyl chloride solution over 10 minutes. while keeping the bulk of the solution at 0 °C. The resulting brown suspension was stirred for one hour at 0 °C. The suspension was then extracted with DCM (4 × 8 mL). The combined organic extracts were washed with saturated aqueous brine (8 mL), dried over Na_2SO_4 and gravity filtered. The solvent was

then removed i*n vacuo* to afford 3-cyano-4-fluorobenzenesulfonyl chloride (504 mg, 74%) as a yellow powder. Melting point: 68-69 °C.

^{1}H NMR (400 MHz, $CDCl_3$): δ (ppm) = 7.46 (dd, *J* = 8.9, 8.1 Hz, 1H, H-5), 8.29 (ddd, *J* = 8.9, 4.5, 2.5 Hz, 1H, H-6), 8.30 (dd, *J* = 5.6, 2.5 Hz, 1H, H-2). EI-MS *m/z* (rel. intensity): 201 (8 $[M\text{-}F]^+$), 184 (39 $[M\text{-}Cl]^+$), 120 (100 $[M\text{-}SO_2Cl]^+$).

4.3.8 4-Nitrophenyl 4-fluoro-3-cyanobenzene sulfonate (12)

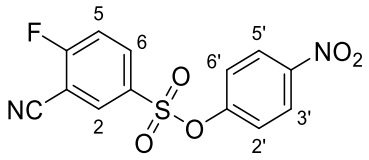

To a yellow solution of 3-cyano-4-fluorobenzenesulfonyl chloride **(11)** (0.605 mg, 2.75 mmol) in dioxane (12 mL) at 0 °C, was added triethylamine (384 µL, 2.75 mmol) and *p*-nitrophenol (385 mg, 2.77 mmol). The yellow solution was stirred for one hour. The resulting orange suspension was vacuum filtered, and the precipitate washed with DCM (5 mL). The filtrate was concentrated *in vacuo* and the residue dissolved in minimal hot ethyl acetate, gravity filtered, and the solvent removed *in vacuo*. The crude orange residue was subjected to silica gel chromatography (eluent: 100% DCM). This afforded 4-nitrophenyl 4-fluoro-3-cyanobenzene sulfonate as a yellow solid (630 mg, 72%). Melting point: 104-105 °C.

^{1}H NMR (400 MHz, $CDCl_3$): δ (ppm) = 7.26 (d, *J* = ~9 Hz, 2H, H-2', H-6'), 7.47 (dd, *J* = 8.8, 8.1 Hz, 1H, H-5), 8.13 (ddd, *J* = 8.8, 4.6, 2.4 Hz, 1H, H-6), 8.22 (dd, *J* = 5.6, 2.4 Hz, 1H, H-2), 8.27 (d, *J* = ~9 Hz, 2H, H-3', H-5'). EI-MS *m/z* (rel. intensity): 322 (9 $[M]^+$), 120 (100 $[M\text{-}SO_2C_6H_4NO_2]^+$).

4.3.9 4-Nitrophenyl 4-(dimethylamino)-3-cyanobenzoate (13)

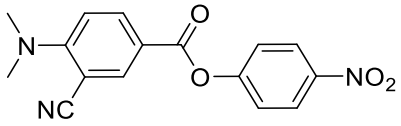

To a stirred solution of 4-nitrophenyl 4-fluoro-3-cyanobenzoate **(5)** (258 mg, 0.90 mmol) in DMSO (5 mL) was added dimethylamine hydrochloride (147 mg, 1.81 mmol) and potassium carbonate (404 mg, 2.93 mmol). The resultant yellow solution was stirred overnight at room temperature. DCM (5 mL) was added to the suspension, which was then washed with ice cold water (3 × 5 mL). The organic layer was then washed with saturated aqueous brine (5 mL), dried over Na_2SO_4, gravity filtered, and dried *in vacuo*. EI-MS analysis of the product showed a mixture of 3-cyano-4-(dimethylamino)-*N*,*N*-dimethylbenzamide (~69 %) and 3-cyano-4-fluoro-*N*,*N*-dimethylbenzamide (~31 %).

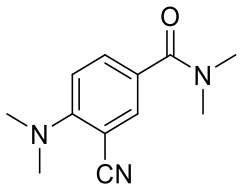

3-cyano-4-(dimethylamino)-*N*,*N*-dimethylbenzamide: EI-MS *m/z* (rel. intensity): 217 (33 $[M]^+$), 173 (100 $[M\text{-}N(CH_3)_2]^+$).

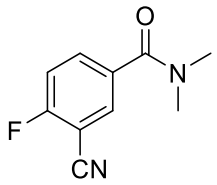

3-cyano-4-fluoro-*N*,*N*-dimethylbenzamide: EI-MS *m/z* (rel. intensity): 192 (21 $[M]^+$), 148 (100 $[M\text{-}N(CH_3)_2]^+$).

4.3.10 Methyl 4-fluoro-3-(trifluoromethyl)benzoate (16)

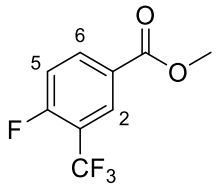

To a stirred ice-cold solution of 4-fluoro-3-(trifluoromethyl)benzoic acid (0.509 mg, 2.45 mmol) in methanol (8 mL) was added acetyl chloride (1.6 mL, 0.22 mol) dropwise. Once the addition was complete, the solution was stirred for 24 hours. The colourless solution was gravity filtered and concentrated *in vacuo.* The light-yellow residue was dissolved in DCM (10 mL) and washed with a saturated aqueous solution of $NaHCO_3$ (2 × 10 mL). The organic layer was then dried over Na_2SO_4, gravity filtered, and dried *in vacuo*. This afforded methyl 4-fluoro-3-(trifluoromethyl)benzoate (321 mg, 59%) as a colourless oil.

^1H NMR (400 MHz, $CDCl_3$): δ (ppm) = 3.95 (s, 3H, OCH_3), 7.28 (dd, *J* = 9.2, 9.2 Hz, 1H, H-5), 8.21 (ddd, *J* = 8.6, 4.8, 2.2 Hz, 1H, H-6), 8.28 (dd, *J* = 6.9, 2.2 Hz, 1H, H-2). EI-MS *m/z* (rel. intensity): 222 (27 $[M]^+$), 191 (100 $[M\text{-}OCH_3]^+$).

4.3.11 Methyl 4-(dimethylamino)-3-(trifluoromethyl)benzoate (17)

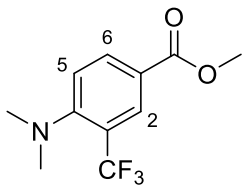

To a stirred solution of methyl 3-(trifluoromethyl)-4-fluorobenzoate **(16)** (646 mg, 2.91 mmol) in DMSO (10 mL), dimethylamine hydrochloride (554 mg, 6.84 mmol) was added followed by potassium carbonate (1.53 g, 11.1 mmol). The suspension was stirred for 48 hours at room temperature. DCM (30 mL) was then added to the yellow suspension, which was then washed with water (3 × 30 mL) and saturated aqueous brine (30 mL). The organic layer was then dried over Na_2SO_4, gravity filtered, and the solvent removed *in vacuo*. This afforded methyl 4-(dimethylamino)-3-(trifluoromethyl)benzoate (535 mg, 74%) as a white powder. Melting point, 48-49 °C

^{1}H NMR (400 MHz, DMSO-d_6): δ (ppm) = 2.87 (s, 6H, $N(CH_3)_2$), 3.84 (s, 3H, OCH_3), 7.34 (d, *J* = 8.7 Hz, 1H, H-5), 8.05 (dd, *J* = 8.7, 2.1 Hz, 1H, H-6), 8.10 (d, *J* = 2.1 Hz, 1H, H-2). EI-MS *m/z* (rel. intensity): 247 (73 $[M]^+$), 246 (100 $[M-H]^+$). Spectral data were in agreement with the literature.[55]

4.3.12 4-(Methoxycarbonyl)-*N*,*N*,*N*-trimethyl-2-(trifluoromethyl) benzenaminium trifluoromethanesulfonate (18)

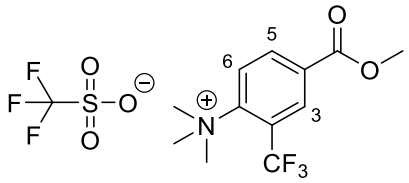

To a stirred solution of methyl 4-(dimethylamino)-3-(trifluoromethyl)benzoate **(17)** (263 mg, 1.06 mmol) in anhydrous DCM (4 mL) under an argon atmosphere was added dropwise methyl trifluoromethanesulfonate (985 mg, 6 mmol) through a rubber septum. The resulting light pink solution was then stirred at room temperature for 70 hours. The resulting brown suspension was vacuum filtered. The white residue was dried *in vacuo* and found to be pure starting material (216 mg, 82%). *Tert*-Butyl methyl ether (4 mL) was slowly added to the brown filtrate to cause precipitation. The fine white precipitate was collected by vacuum filtration and dried *in vacuo*. This afforded 4-(methoxycarbonyl)-*N*,*N*,*N*-trimethyl-2-(trifluoromethyl) benzenaminium trifluoromethanesulfonate (11 mg, 3%). Melting point: 120-122 °C.

^{1}H NMR (400 MHz, D_2O): δ (ppm) = 3.88 (s, 9H, $N(CH_3)_3$), 4.00 (s, 3H, OCH_3), 8.30 (d, 1H, *J* = 9.0 Hz, H-6), 8.46 (dd, 1H, *J* = 8.9, 2.1 Hz, H-5), 8.70 (d, 1H, *J* = 2.1 Hz, H-3). Spectral data were in agreement with the literature.[55]

4.3.13 Methyl 6-chloronicotinate (20)

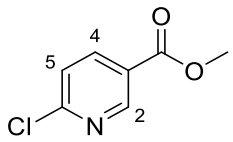

To an ice-cold solution of 6-chloronicotinic acid (512 mg, 3.26 mmol) in methanol (8 mL) was added acetyl chloride (1.6 mL, 0.22 mol) dropwise. Once the addition was complete the yellow solution was stirred for 24 hours. The solution was then vacuum filtered and the collected yellow filtrate dried *in vacuo*. The yellow residue was dissolved in DCM (10 mL) and washed with a saturated aqueous solution of $NaHCO_3$ (2 × 10 mL). The organic layer was dried over Na_2SO_4, gravity filtered, and the solvent removed *in vacuo*. This afforded a yellow powder (316 mg) that was shown by ^{1}H NMR and EI-MS analysis to be a mixture of the desired product methyl 6-chloronicotate (~81 %) and methyl 6-methoxynicotinate (~19 %).

Methyl 6-chloronicotinate: ^{1}H NMR (400 MHz, DMSO-d_6): δ (ppm) = 3.89 (s, 3H, OCH_3), 7.69 (dd, *J* = 8.3, 0.7 Hz, 1H, H-5), 8.31 (dd, *J* = 8.3, 2.4 Hz, 1H, H-4), 8.91 (dd, *J* = 2.4, 0.7 Hz, 1H, H-2). EI-MS *m/z* (rel. intensity): 171 (31 $[M]^+$), 173 (9 $[M+2]^+$), 140 (100 $[M\text{-}OCH_3]^+$). Spectral data were in agreement with the literature.[95]

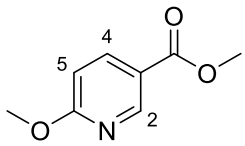

Methyl 6-methoxynicotinate: ^{1}H NMR (400 MHz, DMSO-d_6): δ (ppm) = 3.84 (s, 3H, OCH_3), 3.93 (s, 3H, CO_2CH_3), 6.93 (dd, *J* = 8.7, 0.7 Hz, 1H, H-5), 8.16 (dd, *J* = 8.7, 2.4 Hz, 1H, H-4), 8.74 (dd, *J* = 2.4, 0.7 Hz, 1H, H-2). EI-MS *m/z* (rel. intensity): 167 (62 $[M]^+$), 166 (100 $[M\text{-}H]^+$). Spectral data were in agreement with the literature.[96]

CHAPTER FIVE

Conclusions and Future Directions

This chapter summarises the work performed, and the conclusions drawn from it. It also seeks to discuss the future directions for the work.

5.1 Conclusions and Future Directions

The overall goal of this research is to ultimately develop metabolically stable fluorine-18 labelled peptides that can be efficiently synthesised for use in PET imaging. The specific aims of this thesis were to perform a pilot metabolic stability study on model aromatic amide and sulfonamide analogues using a simple enzyme system and to conduct preliminary studies towards the synthesis of aromatic prosthetic groups that would be highly activated towards both bioconjugation to a peptide at a free amine and subsequent incorporation of [^{18}F]fluoride by nucleophilic substitution.

Chapter 2 presented a metabolic stability study of benzoyl glycine and benzenesulfonyl glycine, as simple amide and sulfonamide model compounds, with pig liver esterase as a model of human carboxylesterase. This study found that both compounds exhibited good stability against the enzyme, however, future work with sample replicates and additional controls, are needed. In addition to this, more sophisticated compounds that incorporate peptides representative of those used in the development of radiopharmaceuticals, and different enzymes such as cytochrome P450s and/or biological media such as mouse plasma, will be conducted for more realistic examination of metabolic stability.

Chapter 3 presented the initial stages of a study for comparing tetramethylammonium (TMA) activated aromatic systems for their ease of peptide conjugation and direct fluorination. This was initially proposed to be achieved using 4-nitrophenyl as an active ester to further activate the target compounds towards peptide conjugation. Unfortunately, the 4-nitrophenyl ester proved to be too active, making it difficult to form the TMA activated aromatic systems. As a result, a new method was developed based upon the synthesis of TMA methyl esters, which could then be fluorinated. Using this method, the synthesis of a TMA bearing methyl ester was successfully trialled. Future work will aim to synthesise all the target TMA bearing methyl ester derivatives described in Chapter 3, with optimised yields such that they can be synthesised in sufficient quantities to pursue fluorination studies to determine which of the compounds show the best activity towards fluorination. This will then help inform the best aromatic scaffolds for future direct fluorination of the glycine ethyl ester and finally peptide conjugates relevant to PET.

REFERENCES

1. Coenen, H. H. *et al.* Fluorine-18 radiopharmaceuticals beyond [18F]FDG for use in oncology and neurosciences. *Nucl. Med. Biol.* **37,** 727–740 (2010).

2. Paans, A. M. J., van Waarde, A., Elsinga, P. H., Willemsen, A. T. M. & Vaalburg, W. Positron emission tomography: the conceptual idea using a multidisciplinary approach. *Methods* **27,** 195–207 (2002).

3. Wood, K. A., Hoskin, P. J. & Saunders, M. I. Positron Emission Tomography in Oncology: A Review. *Clin. Oncol.* **19,** 237–255 (2007).

4. Van de Bittner, G. C., Ricq, E. L. & Hooker, J. M. A philosophy for CNS radiotracer design. *Acc. Chem. Res.* **47,** 3127–34 (2014).

5. Le Bars, D. Fluorine-18 and medical imaging: Radiopharmaceuticals for positron emission tomography. *J. Fluor. Chem.* **127,** 1488–1493 (2006).

6. Molecular imaging targeting peptide receptors. *Methods* **48,** 161–177 (2009).

7. Mullard, A. FDA approvals for the first 6 months of 2016. *Nat. Rev. Drug Discov.* **15,** 523–523 (2016).

8. Reubi, J. C. Peptide Receptors as Molecular Targets for Cancer Diagnosis and Therapy. *Endocr. Rev.* **24,** 389–427 (2003).

9. Okarvi, S. M. Peptide-based radiopharmaceuticals: Future tools for diagnostic imaging of cancers and other diseases. *Med. Res. Rev.* **24,** 357–397 (2004).

10. Langer, M. & Beck-Sickinger, A. Peptides as Carrier for Tumor Diagnosis and Treatment. *Curr. Med. Chem. Agents* **1,** 71–93 (2001).

11. Olberg, D. E. & Hjelstuen, O. K. Labeling strategies of peptides with ^{18}F for positron emission tomography. *Curr. Top. Med. Chem.* **10,** 1669–79 (2010).

12. Patricia Antunes, † *et al.* Influence of Different Spacers on the Biological Profile of a DOTA−Somatostatin Analogue. (2006). doi:10.1021/BC0601673

13. García Garayoa, E. *et al.* Influence of the Molecular Charge on the Biodistribution of Bombesin Analogues Labeled with the [^{99m} Tc(CO) $_3$]-Core. *Bioconjug. Chem.* **19,** 2409–2416 (2008).

14. Eberle, A. N., Mild, G. & Froidevaux, S. Receptor-Mediated Tumor Targeting with Radiopeptides. Part 1. General Concepts and Methods: Applications to Somatostatin Receptor-Expressing Tumors. *J. Recept. Signal Transduct.* **24,** 319–455 (2004).

15. Charron, C. L., Farnsworth, A. L., Roselt, P. D., Hicks, R. J. & Hutton, C. A. Recent developments in radiolabelled peptides for PET imaging of cancer. *Tetrahedron Lett.* **57,** 4119–4127 (2016).

16. Fani, M., Maecke, H. R. & Okarvi, S. M. Radiolabeled Peptides: Valuable Tools for the Detection and Treatment of Cancer. *Theranostics* **2,** 481–501 (2012).

17. Weiner, R. E. & Thakur, M. L. Radiolabeled peptides in oncology: role in diagnosis and treatment. *BioDrugs* **19,** 145–63 (2005).

18. Strauss, H. W. (Harry W. *Nuclear oncology : pathophysiology and clinical applications*. (Springer, 2013).

19. Mease, R. C., Foss, C. A. & Pomper, M. G. PET imaging in prostate cancer: focus on prostate-

specific membrane antigen. *Curr. Top. Med. Chem.* **13,** 951–62 (2013).

20. Maurer, T., Eiber, M., Schwaiger, M. & Gschwend, J. E. Current use of PSMA–PET in prostate cancer management. *Nat. Rev. Urol.* **13,** 226–235 (2016).

21. Giesel, F. L. *et al.* F-18 labelled PSMA-1007: biodistribution, radiation dosimetry and histopathological validation of tumor lesions in prostate cancer patients. *Eur. J. Nucl. Med. Mol. Imaging* **44,** 678–688 (2017).

22. Lucignani, G. Labeling peptides with PET radiometals: Vulcan's forge. (2007). doi:10.1007/s00259-007-0656-2

23. Brechbiel, M. W. Bifunctional chelates for metal nuclides. *Q. J. Nucl. Med. Mol. Imaging* **52,** 166–73 (2008).

24. Liu, S., Park, R., Conti, P. S. & Li, Z. 'Kit like' (18)F labeling method for synthesis of RGD peptide-based PET probes. *Am. J. Nucl. Med. Mol. Imaging* **3,** 97–101 (2013).

25. Honer, M. *et al.* 18F-labeled bombesin analog for specific and effective targeting of prostate tumors expressing gastrin-releasing peptide receptors. *J. Nucl. Med.* **52,** 270–8 (2011).

26. Jacobson, O. *et al.* Rapid and Simple One-Step F-18 Labeling of Peptides. *Bioconjug. Chem.* **22,** 422–428 (2011).

27. Lindner, S. *et al.* Synthesis and in Vitro and in Vivo Evaluation of SiFA-Tagged Bombesin and RGD Peptides as Tumor Imaging Probes for Positron Emission Tomography. *Bioconjug. Chem.* **25,** 738–749 (2014).

28. Litau, S. *et al.* Next Generation of SiFA *lin* -Based TATE Derivatives for PET Imaging of SSTR-Positive Tumors: Influence of Molecular Design on In Vitro SSTR Binding and In Vivo Pharmacokinetics. *Bioconjug. Chem.* **26,** 2350–2359 (2015).

29. Liu, Z. *et al.* Kit-like 18F-labeling of RGD-19F-Arytrifluroborate in high yield and at extraordinarily high specific activity with preliminary in vivo tumor imaging. *Nucl. Med. Biol.* **40,** 841–849 (2013).

30. Pourghiasian, M. *et al.* 18F-AmBF3-MJ9: A novel radiofluorinated bombesin derivative for prostate cancer imaging. *Bioorg. Med. Chem.* **23,** 1500–1506 (2015).

31. McBride, W. J. *et al.* A Novel Method of 18F Radiolabeling for PET. *J. Nucl. Med.* **50,** 991–998 (2009).

32. McBride, W. J., Sharkey, R. M. & Goldenberg, D. M. Radiofluorination using aluminum-fluoride (Al18F). *EJNMMI Res.* **3,** 36 (2013).

33. Miller, P. W., Long, N. J., Vilar, R. & Gee, A. D. Synthesis of ^{11}C, ^{18}F, ^{15}O, and ^{13}N Radiolabels for Positron Emission Tomography. *Angew. Chemie Int. Ed.* **47,** 8998–9033 (2008).

34. Cole, E. L., Stewart, M. N., Littich, R., Hoareau, R. & Scott, P. J. H. Radiosyntheses using fluorine-18: the art and science of late stage fluorination. *Curr. Top. Med. Chem.* **14,** 875–900 (2014).

35. Sánchez-Crespo, A., Andreo, P. & Larsson, S. A. Positron flight in human tissues and its influence on PET image spatial resolution. *Eur. J. Nucl. Med. Mol. Imaging* **31,** 44–51 (2004).

36. Jalilian, A. R. *et al.* One-step, no-carrier-added, synthesis of a18F-labelled benzodiazepine receptor ligand. *J. Label. Compd. Radiopharm.* **43,** 545–555 (2000).

37. Roß, T. L. & Ametamey, S. M. PET Chemistry: An Introduction. in *Basic Sciences of Nuclear Medicine* 65–101 (Springer Berlin Heidelberg, 2010). doi:10.1007/978-3-540-85962-8_5

38. de Goeij, J. J. M. & Bonardi, M. L. How do we define the concepts specific activity, radioactive concentration, carrier, carrier-free and no-carrier-added? *J. Radioanal. Nucl. Chem.* **263,** 13–18 (2005).

39. Ametamey, S. M., Honer, M. & Schubiger, P. A. Molecular Imaging with PET. *Chem. Rev.* **108,** 1501–1516 (2008).

40. Guillaume, M. *et al.* Recommendations for fluorine-18 production. *Int. J. Radiat. Appl. Instrumentation. Part A. Appl. Radiat. Isot.* **42,** 749–762 (1991).

41. Nickles, R. J., Daube, M. E. & Ruth, T. J. An 18O2 target for the production of [18F]F2. *Int. J. Appl. Radiat. Isot.* **35,** 117–122 (1984).

42. Coenen, H. H. Fluorine-18 labeling methods: Features and possibilities of basic reactions. *Ernst Schering Res. Found. Workshop* 15–50 (2007).

43. Jacobson, O. & Chen, X. PET designated flouride-18 production and chemistry. *Curr. Top. Med. Chem.* **10,** 1048–59 (2010).

44. Kim, D. W. *et al.* Facile Nucleophilic Fluorination Reactions Using tert-Alcohols as a Reaction Medium: Significantly Enhanced Reactivity of Alkali Metal Fluorides and Improved Selectivity. (2008). doi:10.1021/JO7021229

45. Furuya, T., Kuttruff, C. A. & Ritter, T. Carbon-fluorine bond formation. *Curr. Opin. Drug Discov. Devel.* **11,** 803–19 (2008).

46. Kim, D. W. *et al.* A New Class of S_N2 Reactions Catalyzed by Protic Solvents: Facile Fluorination for Isotopic Labeling of Diagnostic Molecules. *J. Am. Chem. Soc.* **128,** 16394–16397 (2006).

47. Chun, J.-H. & Pike, V. W. Single-step syntheses of no-carrier-added functionalized [18F]fluoroarenes as labeling synthons from diaryliodonium salts. *Org. Biomol. Chem.* **11,** 6300–6 (2013).

48. Kim, D. W., Jeong, H.-J., Lim, S. T. & Sohn, M.-H. Recent Trends in the Nucleophilic [(18)F]-radiolabeling Method with No-carrier-added [(18)F]fluoride. *Nucl. Med. Mol. Imaging (2010).* **44,** 25–32 (2010).

49. Wester, H. J. & Schottelius, M. Fluorine-18 labeling of peptides and proteins. *Ernst Schering Res. Found. Workshop* 79–111 (2007).

50. Jacobson, O., Kiesewetter, D. O. & Chen, X. Fluorine-18 radiochemistry, labeling strategies and synthetic routes. *Bioconjug. Chem.* **26,** 1–18 (2015).

51. Schirrmacher, R. *et al.* Small Prosthetic Groups in 18 F-Radiochemistry: Useful Auxiliaries for the Design of 18 F-PET Tracers. *Semin. Nucl. Med.* **47,** 474–492 (2017).

52. Richter, S. & Wuest, F. 18F-Labeled Peptides: The Future Is Bright. *Molecules* **19,** 20536–20556 (2014).

53. Zeng, D., Zeglis, B. M., Lewis, J. S. & Anderson, C. J. The growing impact of bioorthogonal click chemistry on the development of radiopharmaceuticals. *J. Nucl. Med.* **54,** 829–32 (2013).

54. Horisawa, K. Specific and quantitative labeling of biomolecules using click chemistry. *Front. Physiol.* **5,** 457 (2014).

55. Becaud, J. *et al.* Direct One-Step ^{18} F-Labeling of Peptides via Nucleophilic Aromatic Substitution. *Bioconjug. Chem.* **20,** 2254–2261 (2009).

56. Tredwell, M. & Gouverneur, V. ^{18} F Labeling of Arenes. *Angew. Chemie Int. Ed.* **51,** 11426–11437 (2012).

57. Höhne, A. *et al.* Organofluorosilanes as Model Compounds for ^{18} F-Labeled Silicon-Based PET Tracers and their Hydrolytic Stability: Experimental Data and Theoretical Calculations (PET=Positron Emission Tomography). *Chem. - A Eur. J.* **15,** 3736–3743 (2009).

58. Liu, Z. *et al.* An organotrifluoroborate for broadly applicable one-step 18F-labeling. *Angew. Chem. Int. Ed. Engl.* **53,** 11876–80 (2014).

59. Diao, L. & Meibohm, B. Pharmacokinetics and Pharmacokinetic–Pharmacodynamic Correlations of Therapeutic Peptides. *Clin. Pharmacokinet.* **52,** 855–868 (2013).

60. Behr, T. M., Gotthardt, M., Barth, A. & Béhé, M. Imaging tumors with peptide-based radioligands. *Q. J. Nucl. Med.* **45,** 189–200 (2001).

61. Mankoff, D. A., Link, J. M., Linden, H. M., Sundararajan, L. & Krohn, K. A. Tumor Receptor Imaging. *J. Nucl. Med.* **49,** 149S–163S (2008).

62. Van Dort, M. E., Jung, Y. W., Sherman, P. S., Kilbourn, M. R. & Wieland, D. M. Fluorine for hydroxy substitution in biogenic amines: asymmetric synthesis and biological evaluation of fluorine-18-labeled beta-fluorophenylalkylamines as model systems. *J. Med. Chem.* **38,** 810–5 (1995).

63. Magata, Y. *et al.* Biologically stable [(18)F]-labeled benzylfluoride derivatives. *Nucl. Med. Biol.* **27,** 163–8 (2000).

64. Pike, V. W. PET radiotracers: crossing the blood-brain barrier and surviving metabolism. *Trends Pharmacol. Sci.* **30,** 431–40 (2009).

65. Hiyama, T. & Yamamoto, H. Reactions of C-F Bonds. in *Organofluorine Compounds* 119–135 (Springer Berlin Heidelberg, 2000). doi:10.1007/978-3-662-04164-2_4

66. Di, L. Strategic approaches to optimizing peptide ADME properties. *AAPS J.* **17,** 134–43 (2015).

67. Barrett, A. J., Rawlings, N. D. & Woessner, J. F. *Handbook of proteolytic enzymes*. (Elsevier Academic Press, 2004).

68. Testa, B., Mayer, J. M. & Wiley InterScience (Online service). *Hydrolysis in drug and prodrug metabolism : chemistry, biochemistry, and enzymology*. (VHCA, 2003).

69. Löser, R. *et al.* Use of 3-[(18)F]fluoropropanesulfonyl chloride as a prosthetic agent for the radiolabelling of amines: Investigation of precursor molecules, labelling conditions and enzymatic stability of the corresponding sulfonamides. *Beilstein J. Org. Chem.* **9,** 1002–11 (2013).

70. Briard, E. *et al.* Single-step high-yield radiosynthesis and evaluation of a sensitive 18F-labeled ligand for imaging brain peripheral benzodiazepine receptors with PET. *J. Med. Chem.* **52,** 688–99 (2009).

71. Fukami, T. & Yokoi, T. The emerging role of human esterases. *Drug Metab. Pharmacokinet.* **27,** 466–77 (2012).

72. Nics, L. *et al.* The stability of methyl-, ethyl- and fluoroethylesters against carboxylesterases in vitro: there is no difference. *Nucl. Med. Biol.* **38,** 13–7 (2011).

73. Testa, B. & Krämer, S. D. The Biochemistry of Drug Metabolism – An Introduction. *Chem. Biodivers.* **4,** 2031–2122 (2007).

74. Weber, M., Frey, W. & Peters, R. Catalytic Asymmetric Synthesis of Spirocyclic Azlactones by a Double Michael-Addition Approach. *Chem. - A Eur. J.* **19,** 8342–8351 (2013).

75. Jursic, B. S. & Neumann, D. Preparation of n-acyl derivatives of amino acids from acyl chlorides and amino acids in the presence of cationic surfactants. A variation of the schotten-baumann method of benzoylation of amino acids. *Synth. Commun.* **31,** 555–564 (2001).

76. DeRuiter, J., Brubaker, A. N., Garner, M. A., Barksdale, J. M. & Mayfield, C. A. In Vitro Aldose Reductase Inhibitory Activity of Substituted N-Benzenesulfonylglycine Derivatives. *J. Pharm. Sci.* **76,** 149–152 (1987).

77. Landowski, C. P., Lorenzi, P. L., Song, X. & Amidon, G. L. Nucleoside ester prodrug substrate specificity of liver carboxylesterase. *J. Pharmacol. Exp. Ther.* **316,** 572–80 (2006).

78. Vine, K. L. *et al.* Targeting urokinase and the transferrin receptor with novel, anti-mitotic N-alkylisatin cytotoxin conjugates causes selective cancer cell death and reduces tumor growth. *Curr. Cancer Drug Targets* **12,** 64–73 (2012).

79. Boellaard, R. *et al.* FDG PET and PET/CT: EANM procedure guidelines for tumour PET imaging: version 1.0. *Eur. J. Nucl. Med. Mol. Imaging* **37,** 181–200 (2010).

80. Al-Faham, Z., Jolepalem, P., Rydberg, J. & Wong, C.-Y. O. Optimizing 18F-FDG Uptake Time Before Imaging Improves the Accuracy of PET/CT in Liver Lesions. *J. Nucl. Med. Technol.* **44,** 70–2 (2016).

81. McGinnity, D. F., Soars, M. G., Urbanowicz, R. A. & Riley, R. J. Evaluation of fresh and cryopreserved hepatocytes as in vitro drug metabolism tools for the prediction of metabolic clearance. *Drug Metab. Dispos.* **32,** 1247–53 (2004).

82. LeCluyse, E. L. & Alexandre, E. Isolation and Culture of Primary Hepatocytes from Resected Human Liver Tissue. in 57–82 (Humana Press, 2010). doi:10.1007/978-1-60761-688-7_3

83. Daumar, P. *et al.* Efficient ^{18} F-Labeling of Large 37-Amino-Acid pHLIP Peptide Analogues and Their Biological Evaluation. *Bioconjug. Chem.* **23,** 1557–1566 (2012).

84. Franck, D. *et al.* Investigations into the synthesis, radiofluorination and conjugation of a new [18F]fluorocyclobutyl prosthetic group and its in vitro stability using a tyrosine model system. *Bioorg. Med. Chem.* **21,** 643–652 (2013).

85. Rebeck, N. T. & Knauss, D. M. Sulfonamide as an Activating Group for the Synthesis of Poly(aryl ether sulfonamide)s by Nucleophilic Aromatic Substitution. *Macromolecules* **44,** 6717–6723 (2011).

86. Ramesh, V. V. E. *et al.* Carboxamide versus Sulfonamide in Peptide Backbone Folding: A Case Study with a Hetero Foldamer. *Org. Lett.* **15,** 1504–1507 (2013).

87. Olberg, D. E. *et al.* One Step Radiosynthesis of 6-[18F]Fluoronicotinic Acid 2,3,5,6-Tetrafluorophenyl Ester ([18F]F-Py-TFP): A New Prosthetic Group for Efficient Labeling of Biomolecules with Fluorine-18. *J. Med. Chem.* **53,** 1732–1740 (2010).

88. Haskali, M. B. *et al.* One-step radiosynthesis of 4-nitrophenyl 2-[18F]fluoropropionate ([18F]NFP); improved preparation of radiolabeled peptides for PET imaging. *J. Label. Compd. Radiopharm.* **56,** 726–730 (2013).

89. Zhang, X., Dunlow, R., Blackman, B. N. & Swenson, R. E. Optimization of 18 F-syntheses using 19 F-reagents at tracer-level concentrations and liquid chromatography/tandem mass

spectrometry analysis: Improved synthesis of [18F]MDL100907. *J. Label. Compd. Radiopharm.* **61,** 427–437 (2018).

90. Woo, L. W. L. *et al.* Dual Aromatase−Steroid Sulfatase Inhibitors. *J. Med. Chem.* **50,** 3540–3560 (2007).

91. Flouret, G. *et al.* Antiovulatory antagonists of LHRH related to antide. *J. Pept. Sci.* **1,** 89–108 (1995).

92. Grewal, G. *et al.* Preparation of heterocyclic sulfonamide compounds as Edg-1 antagonists useful in the treatment of cancer. *World Intellectual Property Organization* (2008).

93. AlJammaz, I., Al-Otaibi, B., Abousekhrah, A. & Okarvi, S. Rapid and one-step radiofluorination of bioactive peptides: Potential PET radiopharmaceuticals. *Appl. Radiat. Isot.* **91,** 17–23 (2014).

94. Zhang, X.-X. *et al.* Comparison of 18F-labeled CXCR4 antagonist peptides for PET imaging of CXCR4 expression. *Mol. Imaging Biol.* **15,** 758–767 (2013).

95. Jung, K. M., Kim, K. H., Jin, J.-I., Cho, M. J. & Choi, D. H. Deep-red light-emitting phosphorescent dendrimer encapsulated tris-[2-benzo[*b*]thiophen-2-yl-pyridyl] iridium (III) core for light-emitting device applications. *J. Polym. Sci. Part A Polym. Chem.* **46,** 7517–7533 (2008).

96. Kaganovsky, L., Gelman, D. & Rueck-Braun, K. Trans-chelating ligands in palladium-catalyzed carbonylative coupling and methoxycarbonylation of aryl halides. *J. Organomet. Chem.* **695,** 260–266 (2010).

APPENDICES

Appendix 1. Representative HPLC Spectra from Chapter 2

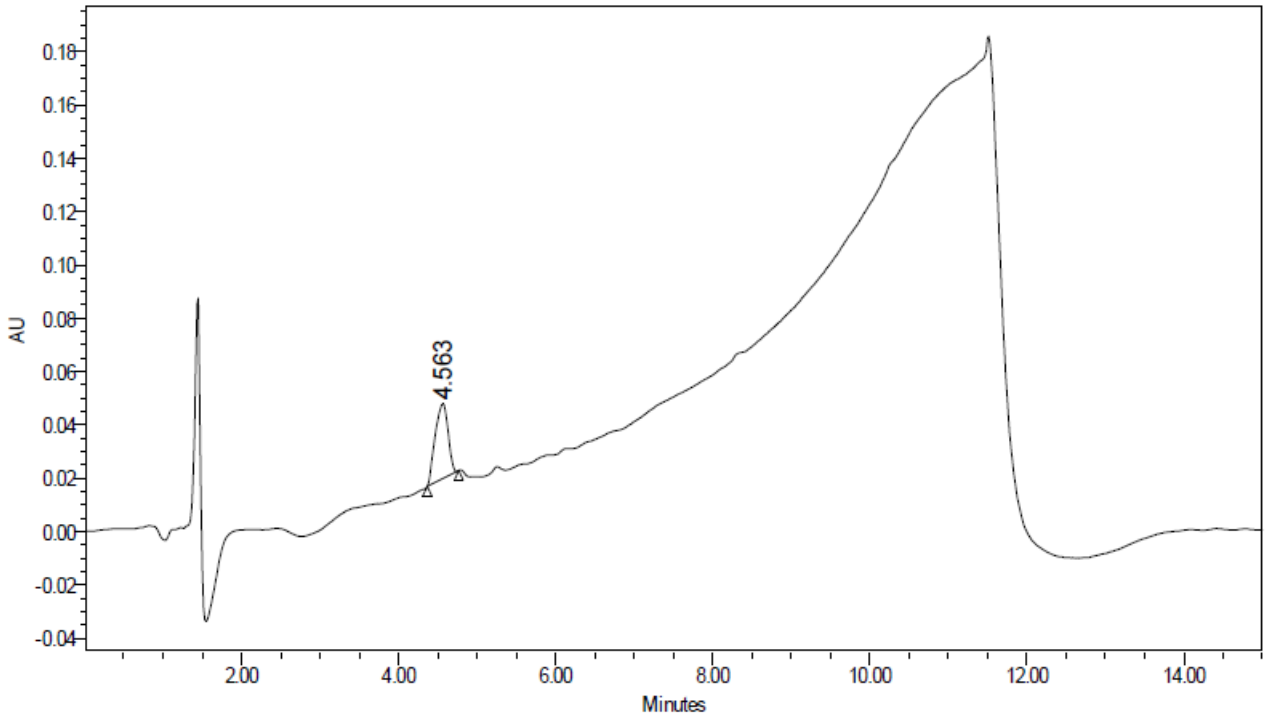

N-Benzoyl glycine 100 U/mL PLE time zero.

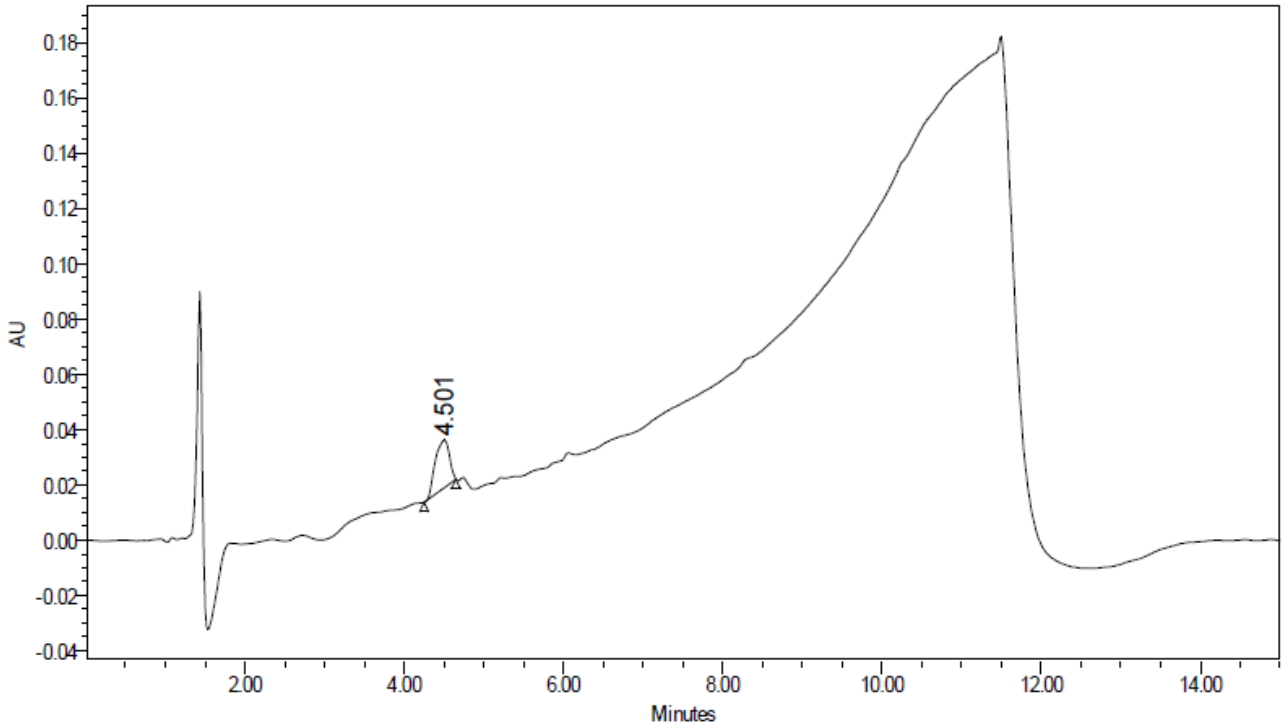

N-Benzoyl glycine 100 U/mL PLE 240 minutes.

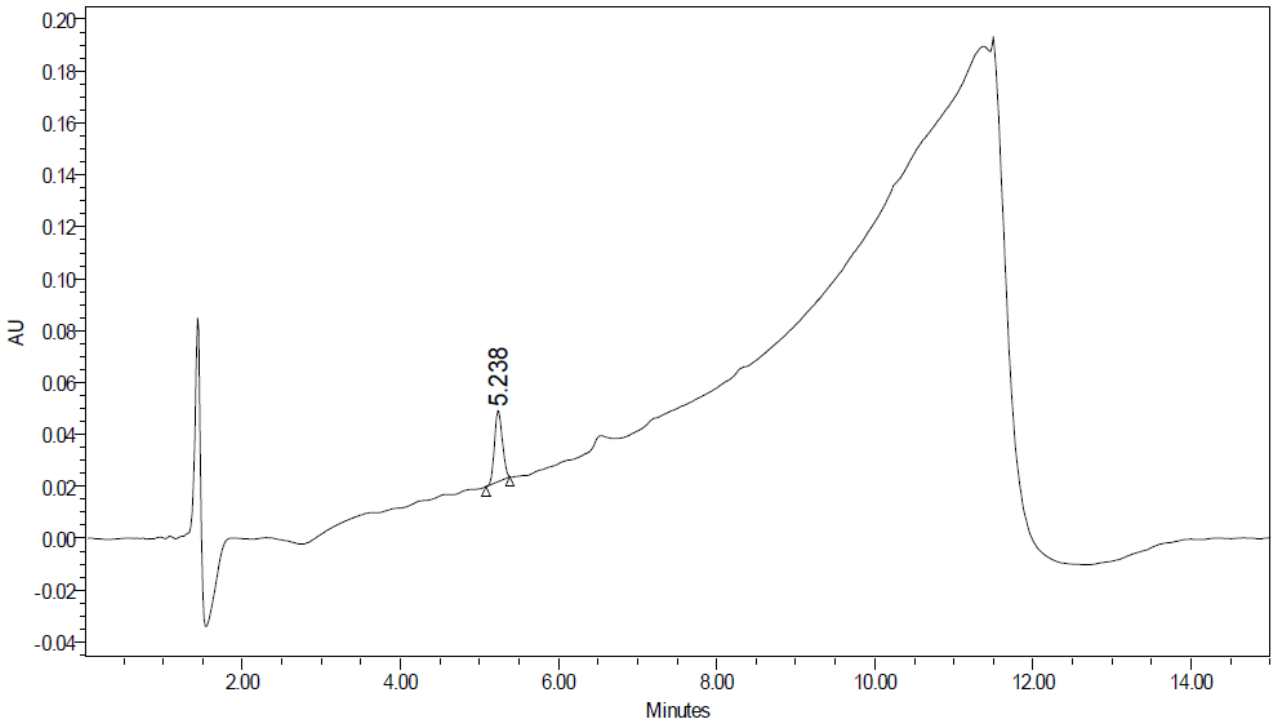

N-Benzenesulfonyl glycine 100 U/mL PLE time zero.

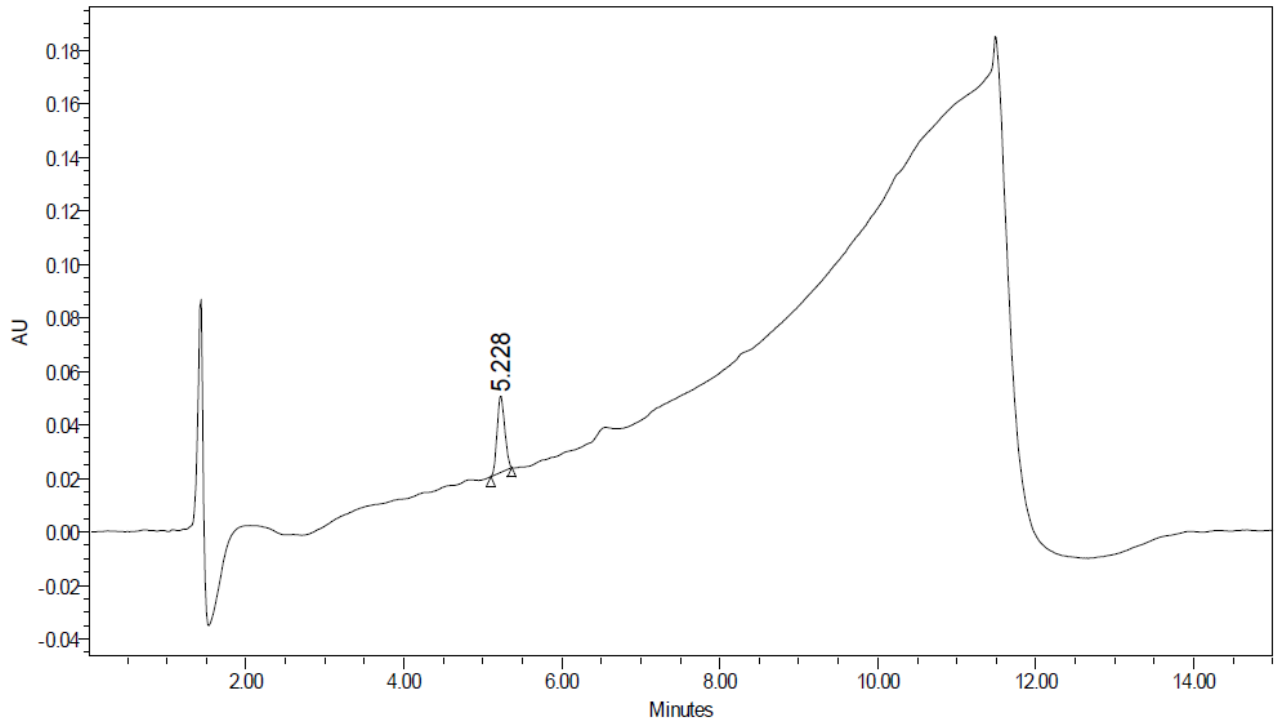

N-Benzenesulfonyl glycine 100 U/mL PLE 240 minutes.